Ultrasonics Sonochemistry 96 (2023) 106441

Contents lists available at ScienceDirect

Ultrasonics Sonochemistry

journal homepage: www.elsevier.com/locate/ultson

Manipulation with sound and vibration: A review on the micromanipulation system based on sub-MHz acoustic waves

Yu Liu [a,b,1], Qiu Yin [c,1], Yucheng Luo [a,1], Ziyu Huang [b], Quansheng Cheng [b], Wenming Zhang [c], Bingpu Zhou [b], Yinning Zhou [b,*], Zhichao Ma [a,*]

[a] Institute of Medical Robotics, School of Biomedical Engineering, Shanghai Jiao Tong University, No.800 Dongchuan Road, Shanghai 200240, China
[b] Joint Key Laboratory of the Ministry of Education, Institute of Applied Physics and Materials Engineering, University of Macau, Taipa, Macau 999078, China
[c] State Key Laboratory of Mechanical System and Vibration, Shanghai Jiao Tong University, Shanghai 200240, China

ARTICLE INFO

Keywords:
Acoustic manipulation
Microfluidics
Sound and vibration
Acoustic radiation force
Acoustic streaming
Acoustic cavitation

ABSTRACT

Manipulation of micro-objects have been playing an essential role in biochemical analysis or clinical diagnostics. Among the diverse technologies for micromanipulation, acoustic methods show the advantages of good biocompatibility, wide tunability, a label-free and contactless manner. Thus, acoustic micromanipulations have been widely exploited in micro-analysis systems. In this article, we reviewed the acoustic micromanipulation systems that were actuated by sub-MHz acoustic waves. In contrast to the high-frequency range, the acoustic microsystems operating at sub-MHz acoustic frequency are more accessible, whose acoustic sources are at low cost and even available from daily acoustic devices (e.g. buzzers, speakers, piezoelectric plates). The broad availability, with the addition of the advantages of acoustic micromanipulation, make sub-MHz microsystems promising for a variety of biomedical applications. Here, we review recent progresses in sub-MHz acoustic micromanipulation technologies, focusing on their applications in biomedical fields. These technologies are based on the basic acoustic phenomenon, such as cavitation, acoustic radiation force, and acoustic streaming. And categorized by their applications, we introduce these systems for mixing, pumping and droplet generation, separation and enrichment, patterning, rotation, propulsion and actuation. The diverse applications of these systems hold great promise for a wide range of enhancements in biomedicines and attract increasing interest for further investigation.

1. Introduction

Attributed to the fast development of micro- and nano-manufacturing, in recent decades, there have been a wide range of technologies emerging for microscale object manipulation. For those micromanipulation technologies aiming at enhancing biochemical analysis, the manipulated objects are usually in a fluidic environment. This attracts plenty of research interest towards the field of microfluidics, which refers to the dynamics and precise manipulation of microscale fluid. Due to its small sample volume and the automation compared to the conventional biochemical analysis, the microfluidic platforms have the advantages of low cost, wide tunability and portable sizes [1-15].

Aiming at these microfluidic manipulations, a variety of technologies have been developed, which can be categorized by their applied physical fields, e.g. electrical [16-19], optical [20-22], magnetic [23,24], acoustic [25-27], thermal [28,29], hydrodynamical [30,31] and combinational methods [32,33]. These methods show their promises in sample treatment between the sample collection and analysis, such as mixing, synthesis, separation, and enrichment. The exploitations of the various control methods usually involve the consideration of their merits and limitations. For example, the electrical method commonly utilizes the electrostatic or dielectrophoretic force for near-field particle manipulation. The size of the manipulated object has a wide range from $\sim$ 10 nm to $\sim$ 100 μm. However, the distance between the manipulated objects and the electrodes is limited due to its near-field identity, which might impede its application. The optical tweezers are shown as promising tools for nanoparticle or cell manipulation, while the high optical intensity at focus and the resultant thermal effect might cause potential damage to the bio-samples. Magnetic methods are widely used in the

* Corresponding authors.
E-mail addresses: ynzhou@um.edu.mo (Y. Zhou), zhichaoma@sjtu.edu.cn (Z. Ma).
[1] These authors contributed equally to this work.

https://doi.org/10.1016/j.ultsonch.2023.106441
Received 27 February 2023; Received in revised form 6 May 2023; Accepted 12 May 2023
Available online 13 May 2023

high throughput separation and enrichment of microparticles. Whereas, it requires the magnetic properties or magnetic labelling of the samples. Acoustic methods show the advantages of incomparable good biocompatibility and simple setup. The acoustic waves can transmit through the various mediums between the solids and liquids, thus providing flexibility among a vast range of positions between the manipulated micro-objects and the acoustic source. In the recent decade, acoustic micromanipulation has been attracting growing research interests and has offered promising tools for biochemical analysis [34-36].

Some recent reviews have highlighted the fast development of acoustic micromanipulation [6,37-40]. The acoustic waves have a very broad range of frequencies from below 10 Hz to over 1 GHz, which results in a wide-range review across different acoustic and hydrodynamic effects, acoustic sources, and micro-fabrications. In contrast, this review is mainly concerned with acoustic waves at a relatively low-frequency range which is below 1 MHz. In comparison to high-frequency Microelectromechanical Systems (MEMS) devices, the sub-MHz acoustic micromanipulation systems commonly require acoustic supply with low-cost and simply produced acoustic components such as buzzers, piezoelectric plates, and speakers. Moreover, the acoustic wavelengths in the medium are larger than one millimeter when the system works at the sub-MHz range, which matches the common size of the microfluidic channels or chambers. This results in a good homogeneity of the acoustic energy distribution, which is advantageous to high throughput and parallel manipulation. In addition, if at the same acoustic intensity, the low-frequency acoustic waves have a higher vibration amplitude than the high-frequency ones. The larger vibration amplitude leads to a higher possibility for cavitation, which has been applied in sonochemistry for synthesis and mixing [38,41]. The low-frequency acoustic waves could introduce the acoustic cavitation effect as a new mechanism to the microfluidic system.

This review complements other recent reviews on the topic of acoustic micromanipulation [6,37-40]. In contrast to reviewing the whole frequency range of acoustic waves, we focus on the recent breakthroughs in microfluidic manipulation with low frequencies (lower than 1 MHz), aiming to illustrate their promising applications in a variety of life science, biomedical applications and chemical reaction controls. Here, we review acoustic micromanipulations based on sub-MHz acoustic waves concerning their operation principles and applications (Fig. 1). In session 2, we introduce three basic principles (sessions 2.1–2.3) and setups (session 2.4) for the acoustic micromanipulation at the sub-MHz frequency range, including acoustic radiation force, acoustic streaming effect and acoustic cavitation. In session 3, we present a literature review of this field, which is categorized according to their applications, i.e. mixing (3.1), pumping and droplet generation (3.2), separation and enrichment (3.3), patterning (3.4), rotation (3.5), propulsion and actuation (3.6), other application (3.7). Finally, we discuss the future perspectives and outlooks on microparticle manipulation with sub-MHz acoustic waves.

2. Basic mechanisms

While using acoustic waves for micromanipulation, one of the fundamentals is the conversion from acoustic energy to the movement of the micro-objects. This relies on some nonlinear acoustic effects that induce the momentum change of the microparticles or their environments. In this session, we describe three basic acoustic effects that are commonly used in micromanipulation based on sub-MHz acoustic waves, namely acoustic radiation force, acoustic streaming, and acoustic cavitation.

2.1. Acoustic radiation force

The acoustic radiation force (ARF) is a time-averaged force that exerts on the interface between two media with different acoustic properties, due to the scattering and absorption of the acoustic energy. It can be experienced by surfaces, structures, or particles exposed to acoustic waves. The evaluation of acoustic radiation relies on integrating the time averaged stress tensor in the total acoustic field over the closed time-varying surfaces based on the stress tensor proposed by Brillouin [42] and far-field scattering theory,

$$F_{ARF} = -\oint_s \left[\left(\langle p^2\rangle/2\rho_0 c_0^2 - \langle|\boldsymbol{v}|^2\rangle\rho_0/2\right)I + \rho_0\langle \boldsymbol{vv}\rangle\right]\cdot ds \quad (1)$$

where $\oint_s$ means the surface integral, $ds = nds$ represents direct away from the obstacle. The time average over the acoustic wave period is denoted by the angled brackets $< \cdots >$ and I is the unit tensor. ρ_0 and c_0 is the density and sound speed in the fluid respectively. The total acoustic pressure and velocity generated from the sum of waves incident and scattered by obstacles are presented by p and $\boldsymbol{v}$. The equation illuminates that the acoustic force can be influenced by the acoustic properties of the particle and fluid.

Generally, equation (1) is commonly used to analyze acoustic radiation force induced by complex acoustic fields and non-spherical particles. For the situation of manipulation of microparticles in the sub-MHz acoustic field, the radius of particle a is much smaller than the acoustic wavelength, which is called Rayleigh particle ($a \ll \lambda$), such as cells. Gor'kov [43] derived an equation to calculate the ARF on Rayleigh

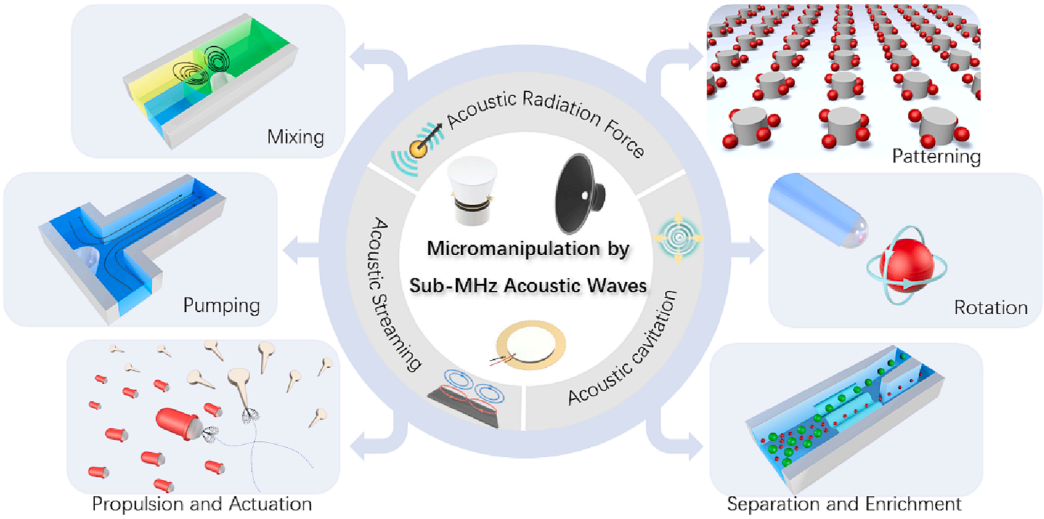

Fig. 1. Micromanipulation based on sub-MHz acoustic systems.

particle in the position where the acoustic field has a standing wave character or spatial gradient of acoustic wave energies:

$$F = -\nabla U \tag{2}$$

where U presents Gor'kov force potential and is expressed using the acoustic pressure and velocity as:

$$U = (4\pi a^3/3)\left[f_1\langle p^2\rangle/2\rho_0 c_0^2 - 3f_2\rho_0\langle|\boldsymbol{v}|^2\rangle/4\right] \tag{3}$$

where $4\pi a^3/3$ is the volume of the particle and the scattering coefficients are given by:

$$f_1 = 1-\rho_0 c_0^2/\rho_p c_p^2, f_2 = 2\left(\rho_p-\rho_0\right)/(2\rho_p+\rho_0) \tag{4}$$

where ρ_p and c_p are the density and the longitudinal wave velocity of the particle; the scattering coefficients f_1 and f_2 represent the monopole and dipole coefficients, respectively.

Under the standing wave generating in virtue of the reflection layer which parallels the transducer, suspended particles will be positioned to a nodal or antinodal position via the acoustic radiation force (F_{ARF}), expressed as:

$$F_{ARF} = -\pi p_0^2\beta_m V_p \Phi(\beta,\rho)\sin(4\pi x/\lambda)/2\lambda \tag{5}$$

where V_p means particle volume, p_0 is acoustic pressure and Φ presents acoustic contrast factor [44]. Φ is determined by the density of particle (ρ_p) and medium (ρ_m), also the compressibility of particle (β_p) and medium (β_m), listed as:

$$\Phi(\beta,\rho) = \left(5\rho_p - 2\rho_m\right)/\left(2\rho_p+\rho_m\right) - \beta_p/\beta_m. \tag{6}$$

The acoustic contrast factor measures the difference in density between the particle and fluid media. With the great density differing of particles and fluid, the acoustic contrast factor increases. The force potential is in turn proportional to the acoustic contrast factor Φ, and the ARF strength increase, too. In comparison, the cell will experience lower ARF than solid particles in a fluid environment because it contains plenty of water. The positive and negative acoustic contrast factor is determined by particle material thus the direction of ARF changed. For example, in the same acoustic field and fluid, silica particle has positive acoustic contrast ($\Phi > 0$) which will move against spatial pressure gradient and enrich in the pressure node (where $P = 0$), while the bubble has negative acoustic contrast ($\Phi < 0$) which will migrate to the antinode (where $P = \max$).

In addition to the ARF induced by the momentum transfer from the primary acoustic field to the particle, which is commonly called primary ARF, the particle vibration also radiates and induces ARF to the adjacent particles, which is known as secondary ARF or Bjerknes force. It was first described by Vilhelm Bjerknes in his 1906 Fields of Force [45]. Compared to the solid particles, the compressible bubbles can be excited with more oscillation displacements at resonance, thus the Bjerknes forces are more obviously observed from bubble clusters. Attraction and repulsion can arise from Secondary Bjerknes force by adjusting bubble size and the acoustic field [46]. When bubbles aggregate in the low acoustic pressure region, secondary Bjerknes force can be applied in patterning bubbles. The Bjerknes force can be experienced by compressive particles, like polymer particles.

2.2. Acoustic streaming

Acoustic streaming is a nonlinear acoustic effect which converts acoustic energy to fluid flow [47]. In the aspect of particle manipulation, acoustic streaming flows will exert a drag force on the particles to translate or rotate them.

There are three main kinds of acoustic streaming phenomena: Eckart streaming, Schlichting streaming and Rayleigh streaming. Eckart streaming occurs in a bulk fluid due to acoustic attenuation during propagation. The absorbed energy from the acoustic waves attenuation gives rise to flow [48]. Schlichting streaming is driven by shear within the viscous boundary layer next to a solid wall [3,49]. Rayleigh streaming appears out of the viscous boundary layer and is driven by its shear of it in the bulk fluid [50]. The last two types of streaming are commonly used for manipulating microparticles in the fluid under a sub-MHz acoustic source.

Taking a common example in this review, when structures (channel walls, micropillars, microbubbles or sharp edges) are excited inside the microfluidic channel and immersed in the fluid, the steep velocity gradient induces inner (Schlichting) streaming inside the boundary layer, which is caused by vibration energy dissipation. Then outer (Rayleigh) streaming vortices will generate in the nearby bulk fluid. The suspended particles in the microfluid channel will experience a drag force from the acoustic streaming and thus be manipulated, which is given by:

$$F_D = 3\pi\mu d\boldsymbol{u} \tag{7}$$

where μ is the dynamic viscosity, d refers to the particle diameter and $\boldsymbol{u}$ is the velocity of surrounding flows relative to that of the particle. Obviously, the drag force is proportional to the particle size. The properties of the fluid (viscosity) also influence streaming and particle manipulation. More importantly, outer steady Rayleigh streaming motion will depend on the microstructure (in the microfluid channel or microparticle). When the microstructure is excited on resonance, the vibration is maximal, together with the strongest Rayleigh streaming. Generally, the high-aspect-ratio (like sharp edge) structures provide stronger streaming than low-aspect-ratio structures when the acoustic intensity is at the same level. At last, the acoustic source is also one crucial factor for manipulating particles, the key acoustic parameters include frequency, amplitude, and vibration mode.

2.3. Acoustic cavitation

Acoustic cavitation describes a phenomenon when the negative acoustic pressure reaches a certain level that vaporized the liquid or drags the dissolved gas for forming cavities in the liquid. The bubbles generally grow up on the solid boundary with rough surfaces or sprint from microcavities suspended in the fluid. Cavitation can be classified as two models based on the follow-up development of the cavity. The mechanical index (MI) [51] is used for indicating the strength of the cavitation effect:

$$MI = P_{np}/\sqrt{f_0} \tag{8}$$

where P_{np} is the peak negative pressure in an acoustic wave and f_0 means the frequency. MI unit is $\mathrm{MPa}/\sqrt{\mathrm{MHz}}$. At High acoustic power ($\mathrm{MI} > \sim 0.7$), a void or bubble in a liquid will violently oscillate to rapidly collapses, thus producing a shock wave. This is known as inertial cavitation [52]. Bubble collapse can provide strong mechanical and thermal stimuli, thus the temperature can reach several thousand kelvins temporarily and pressure on the order of tens of megapascals. Therefore it is a strong approach to transfer acoustic energy into the fluid. This effect is easier to realize at a lower frequency, where the strong negative pressure duration of each cycle is longer than the higher frequency. At a slightly higher mechanical index ($0.1 < \mathrm{MI} < 0.4$), a bubble in a fluid is forced to oscillate in size or shape due to an acoustic field, which is referred to as non-inertial cavitation. Hence, the vibration of the embedded bubble in the structure generating streaming can be called cavitation, too. For utilizing non-inertial cavitation in acoustic manipulation more easily, optothermal [53], electrochemical [54,55] or direct inlet gas [56] is induced to generate bubbles [57]. While at low power ($\mathrm{MI} < 0.1$), the bubble linearly scatters the acoustic wave which is usually not considered in acoustic manipulation [58].

Acoustic cavitation is widely adopted in the sub-MHz acoustic

micromanipulation system. The cavitation-induced flow profile, whether by inertial or non-inertial cavitation, is an enhancement to the mass exchange within the fluid, thus becoming an approach for fast mixing and chemical synthesis. The cavitation-induced momentum transfer can provide propulsion to the microparticles or mobile microstructures, thus working as a new actuation method for micromechanical systems. Acoustic cavitation can also be used to tune the permeability of some biological barriers, such as cell membrane, blood–brain barrier, and blood-spinal cord barrier. When the cavitation is at certain high intensity, the cells or thrombus can be lysed. A similar mechanism can also be applied in microreactors for chemical reactions, water purification, and suspended particle degradation in a colloidal liquid compound.

2.4. System setups

There are two central elements in the sub-MHz acoustic micromanipulation system: the acoustic sources and the microfluid environments. Thus, the system setups can commonly be categorized based on the relative positions of these two elements, though the system parameters and the applications may differ. The relative positions of the acoustic source and fluid also determine the wave propagation approach from the former to the latter. Based on this criterion, this review categorizes the sub-MHz acoustic micromanipulation systems into three types: guided wave propagation, transmissive wave propagation and standing wave (Fig. 2). For guided wave propagation, the acoustic wave propagates along the length of the plate. The examples (Fig. 2a) are the side-affixed acoustic source near the microchamber, vibration stage with plate pane and bonded acoustic source at one side of a probe. For direct transmission, the acoustic wave propagates along the thickness of the plate or directly interact with particle through fluid (Fig. 2b). One of the examples is a speaker positioned beneath a microchamber, where the vibration from the speaker directly transmits to the fluid environment. For reflected wave, the acoustic wave reflects and generate a standing wave between two reflective surfaces. An example is positioning a reflective plate in parallel with a plane acoustic transducer (Fig. 2c), where the acoustic waves generated from the latter transmit into the fluid and reflect at the former, thus interfering as a standing acoustic field. Due to the simple setup of an acoustic source, sub-MHz acoustic manipulation devices can be assembled easily. By putting the acoustic source in different positions of the devices and exciting selectively, multiple vibration modes can be realized.

3. Applications of the sub-MHz acoustic micromanipulation system

3.1. Mixing

Effective control over the concentration or gradient of certain chemical species in microfluidic systems is essential for successful biochemical analysis [59], and particle synthesis [60]. The miniaturized fluid geometry in microfluidic systems offers a superior surface-to-volume ratio compared to macro chemical reactors, resulting in improved heat and mass transfer. However, the small fluid dimensions also result in a low Reynolds number (typically smaller than 0.1) [59,61]. A low Reynolds number results in limited turbulent mixing. Under the laminar flow condition, species diffusion dominates the mixing process, yet it is inherently slow. To enhance the mixing efficiency in microfluidic systems, researchers have explored various strategies like magnetic [62], optical [63], electrical [64], hydrodynamical [65] and acoustic [66] methods. Among these, sub-MHz acoustic methods are advantageous due to label-free, low cost and wide-tunability, thus have been widely applied in microfluidic mixing [59,67].

3.1.1. The sub-MHz acoustic micromixer

Several early studies have demonstrated that vibrations in microfluidic channels can induce acoustic streaming, thereby expediting the exchange of chemical species. For example, Yang et al. [73] reported a microfluidic mixer actuated by a 60 Hz transducer placed under the microchamber. It accelerated the mixing of urine solution and water flowing at an mL min^{-1} scale. Neild et al. [74] showed that swirling flow caused by harmonically vibrating fluid boundaries enhanced the mixing. In the later studies, the microstructures (e.g. micropillars [75], sharp edges, cavitation bubbles) were introduced into the microfluidic channels to achieve more localized streaming control. The resonant microstructures induce greater pressure and velocity fluctuations within the fluid, leading to rapid and homogenized mixing. In general, bubble vibration-induced streaming occurs at resonance frequency $>$ 10 kHz, while sharp edge vibration-induced streaming occurs at resonance frequency $<$ 10 kHz. As shown in Fig. 3a, Ahmed et al. [68] reported a microfluidic mixer based on bubble-induced acoustic streaming effects. The cavity structures were fabricated on both sides of the microchannel to trap air, and the piezo transducer is bonded with the microchannel onto a petri dish to supply acoustic energy for the vibrating bubble. By utilizing this design, deionized water and ink were mixed $<$120 ms at a frequency of 81.4 kHz. Similar mixer devices were made by Huang et al. [76] that the embedded bubbles are replaced by sharp edges to achieve rapid mixing under 4.5 kHz. Except for the structure placed on both sides of the microchannel, a single structure, such as a horse-shoe structure for trapping air bubbles [41] or microneedles [77], can also enable fast mixing.

Despite the capability for fast mixing, acoustic micromixers are faced with a challenge that restricts their effective application in industrial settings – low throughput capacity. Generally, the majority of these acoustic micromixers can only achieve a throughput level of 1–100 μL min^{-1} [41,76]. Thus, improving throughput level is vital for the successful utilization of acoustic micromixers in practical applications. The research conducted by Le et al. prioritized achieving high throughput performance in acoustic micromixers, resulting in a large flow rate of 8 mL/min through the utilization of a star-shaped micromixer with an oscillating frequency of up to 620 kHz. [60]. To solve the limitation that

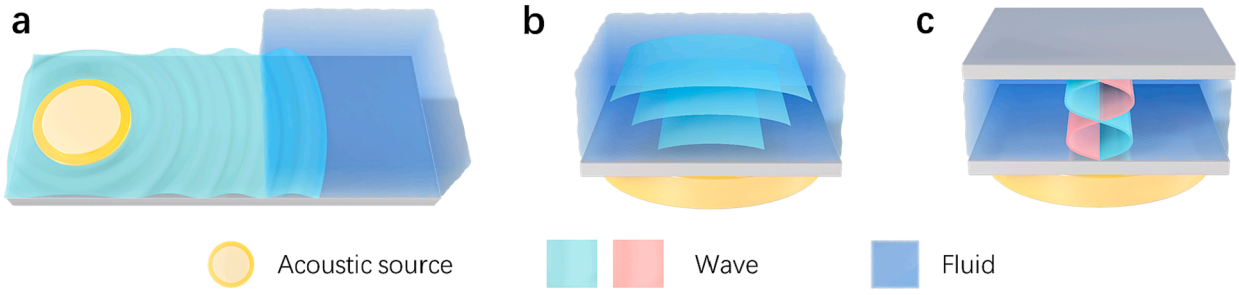

Fig. 2. The schematics for the three types of sub-MHz acoustic manipulation systems (categorization based on the relative positions of the acoustic source and the fluid). (a) guided wave propagation (b) transmissive wave propagation (c) standing wave.

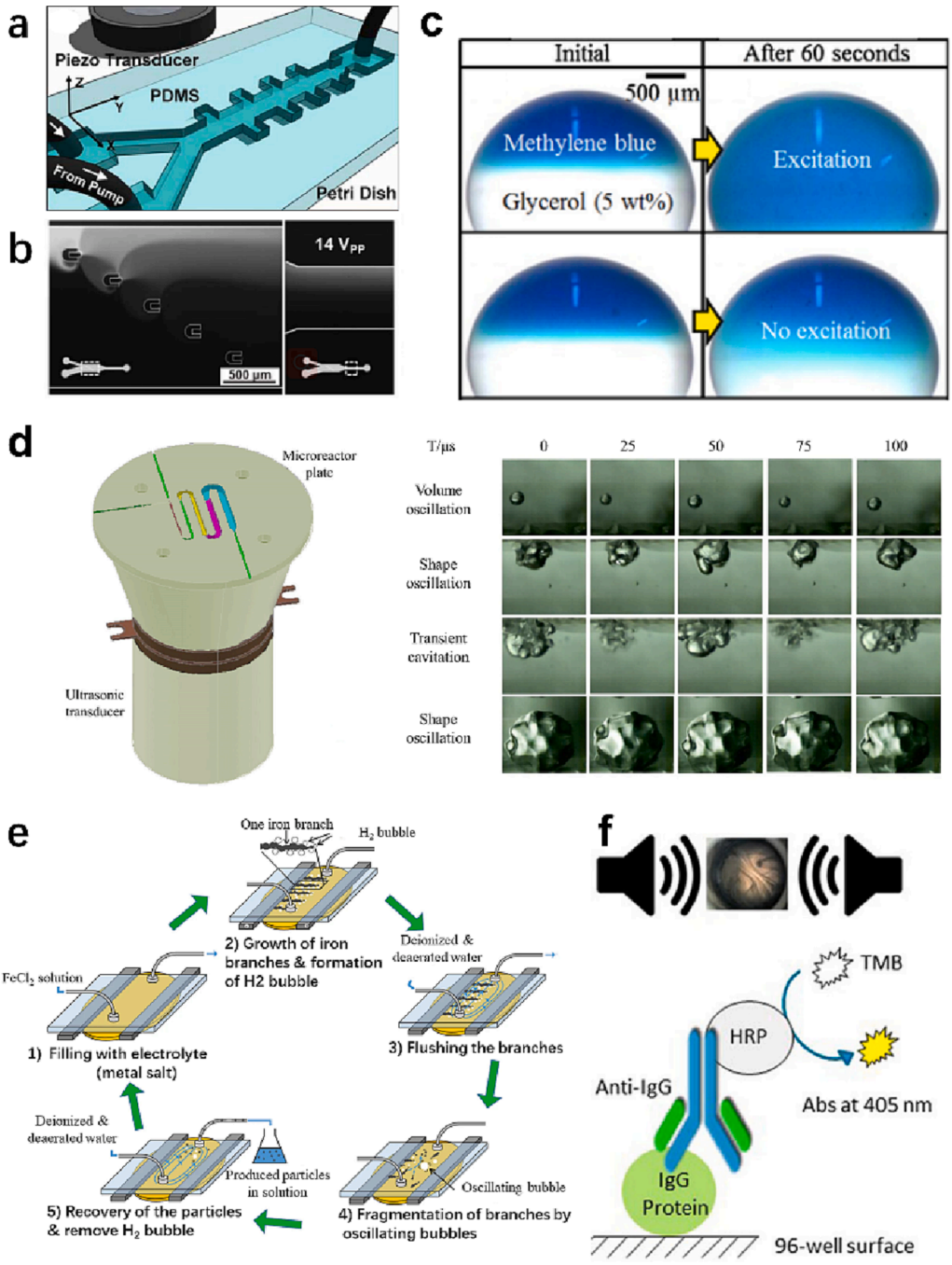

Fig. 3. Mixing in sub-MHz acoustic microsystems. (a) The sub-MHz acoustic waves are generated from the Piezo transducer, transmit through the substrate and coupled into the microfluidic channel. The microstructures vibrate at their resonance and enhance the mixing inside the microfluidic channel. Reproduced from reference [68]. Copyright 2009, Springer Nature Limited. (b) The enhanced mass exchange can also be used in controlling the concentration gradient profiles. Reproduced from reference [69]. Copyright 2013, Royal Society of Chemistry. (c) Acoustic streaming in droplets and the comparison between excited by or not by the sub-MHz vibration. Reproduced from reference [70]. Copyright 2016, Elsevier B.V. (d) The micromixing under intense acoustic energy (10 W) based on inertial cavitation. The microbubbles form and collapse within microchannels, which results in a fast-mixing process of 3 mL min^{-1}. The scale bar is 500 μm. Reproduced from reference [71]. Copyright 2019, Elsevier B.V. (e) Representation of the particle synthesis based on sub-MHz acoustic microsystem. Reproduced from reference [54]. Copyright 2019, Springer Nature Limited. (f) An example of biosensing based on the micromixer: increasing the antibody-antigen binding rate in immunoassays. Reproduced from reference [72]. Copyright 2015, Springer Nature Limited.

inherently designs normally restricted the operational throughput, Bachman et al. [78] developed an acoustic mixing device capable of handling flow rates ranging from 20 to 2000 μL min^{-1} by oscillating the sharp edges combined with the tesla valve structure at the frequency of 5.3 kHz.

Accurate control over microenvironments within microfluidic devices is another crucial aspect of micromixers besides mixing efficiency. Generating tunable chemical gradients has practical implications for the characterization of dynamic biological and chemical processes, such as resolving the dynamics of cellular response to a chemical microenvironment [34,79]. A chemical gradient generator was developed by Ahmed et al. [69] for generating both static and pulsatile chemical gradients using acoustically activated bubbles arranged in a ladder-like configuration, as shown in Fig. 3b. Huang et al. [80] also developed a spatiotemporally controllable gradient generator by manipulating the driving voltage and actuation time of a piezoelectric transducer located in sharp-edge array structures embedded in a microchannel. They further designed the chemical signal generators with bubble [81] and sharp edges [82] structure, respectively. In addition to the chemical gradient within microchannels, the vibration-enhanced streaming also works in a sessile droplet. Lee et al. [70] selectively mixed two 6 μL magnetic droplets based on their size by inducing acoustic streaming within the droplet's liquid–gas interface using 249 Hz acoustic vibration. Mixing was completed within 60 s with acoustic excitation, while no mixing occurred without it (Fig. 3c). A novel approach has also been proposed by Won et al. [83] for manipulating and blending droplets in an electrowetting microfluidic platform using acoustic excitation.

The aforementioned acoustic mixers primarily depend on acoustic streaming effects. In contrast, Chen et al. [71] demonstrated that inertial acoustic cavitation can enhance mass/heat transfer, as depicted in

Fig. 3d. The intense acoustic waves generated from the Langevin transducer transmitted into the microchannel, leading to the formation of cavitated microbubbles. The microbubbles within the microchannels undergo violent oscillation and collapse, accelerating the Toluene conversion reaction. The group also showcased the utilization of comparable mechanism in gas–liquid, liquid–liquid mass transfer intensification [84-88], as well as emulsification [89,90].

3.1.2. Material synthesis

The significance of nanomaterial synthesis technology lies in the vast potential of nanoparticles in areas such as medical diagnosis, imaging, and therapeutics. However, Conventional bulk mixing and most microfluidic approaches faces difficulties in synthesizing reproducible and controlled particles. With the capability to manipulate the local microfluidic environment, the sub-MHz acoustic micromixer can synthesize nanoparticles accurately and efficiently [60,91-93]. For example, Rasouli et al. [94] utilized the combination of vibrated sharp edges and cavitation bubbles array to produce microstreaming, which enabled swift synthesis of polymeric nanoparticle and liposome. Zinc Oxide Nanoarrays are a type of nanostructure composed of zinc oxide nanowires or nanorods that are arranged in an array-like pattern. It has unique physical and chemical properties that make them attractive for various applications in electronics, optoelectronics, energy harvesting, sensing, and biomedical devices. By applying a sharp edge base acoustic micromixer, Zinc Oxide Nanoarrays can be grown in situ with robust and customizable geometries [95,96]. These methods rely on structure-vibration-induced microstreaming to enhance mixing and control particle synthesis and nanoarray growth, while some others employ oscillating bubbles generated from a chemical reaction to enhance mixing and produce nanoparticles. For example, an electrochemical method was employed by Iranzo et al. [54] to cultivate iron branches and generate H_2 bubbles inside micromixer. While streaming induced by vibrating bubbles fragment branches, dendritic particles with a very high specific surface, ~ 2 μm long and ~ 1 μm wide, and needle-like particles, ~ 200 nm long and ~ 20 nm in diameter (broken tertiary dendrites) were produced, as shown in Fig. 3e.

3.1.3. Biosample mixing for analysis

Acoustic micromixer plays an important role in biological analysis, particularly in bio-sensing, as it promotes the efficacy and sensitivity of biochemical reactions [77,97]. Moreover, it can greatly save sample amounts and reduce the detection time. According to a recent report, multiple cancer biomarkers were simultaneous detected within minutes using an acoustic micromixer integrated magnetic-based single-bead trapping technique, in which acoustic microstreaming was generated for minimizing the diffusion length scales [98]. Conde et al. [99] conducted a study where they compared the performance of hybrid micromixer and bench protocol for cell-free DNA extraction in 100 μL plasma samples using a commercial kit based on magnetic beads. The results shows that the hybrid micromixer was able to significantly outperform the bench protocol in terms of efficiency and effectiveness. Gao et al. [72] increased the antibody-antigen binding rate in immunoassays (ELISA) by using a well plate micromixer (Fig. 3f). The results showed the acoustic micromixer achieved an equivalent binding level in 9 mins, compared to 45 mins in a standard platform rocking mixer. In addition to accelerating the biochemical reaction, the acoustic micromixer exhibits potential for bio-sample processing. This includes liquefaction or emulsification of viscous bio-samples, which is the fundamental step for subsequent bioanalysis or medical diagnostics, like analyzing bacteria and causative agents. The sub-MHz acoustic micromixer has led to advancements in developing portable and fast microchip platforms. Human-resource samples (stool [100], sputum [101]) have been homogeneously liquified at a throughput rate of 30 μL min^{-1} using this technology.

As above, sub-MHz acoustic mixers express brilliant capability in enhancing gradient control, synthesizing, and sample processing. The precise control over microenvironments can improve the analysis by reducing the experiment duration consumption and providing more controllable conditions, such as the species concentration, pH, and microparticle characteristics. Therefore, sub-MHz acoustic micromixing systems greatly aids in advancing biochemical research and medical diagnostics.

3.2. Pumping and droplet generation

At the micro- to nano-scale, precise controlling over fluid is necessary for various microfluidics application, including biochemical analysis, drug delivery, and diagnostics. To realize these operations, microfluidics devices have employed diverse external energy inputs, such as electrical, magnetic, optical and acoustic approaches [107-111]. Among them, acoustic methods exhibit the advantages of good compatibility, high integration and wide adjustability. And sub-MHz acoustic attracted increasing research interest for its low-cost, simplicity as well as good homogeneity distribution of acoustic energy. Here, we categorize the fluid control into two groups on account of the functions: pumping and droplet generation. Generally, the sub-MHz acoustic fluid pumping systems work by inducing acoustic streaming flow through oscillating different structures: microbubbles [102,112-114], and sharp-edge structures [103,104,115,116]. Acoustic droplet generation systems work based on acoustic radiation force [105,117] and acoustic streaming [106].

Acoustically activated microbubbles induce resonance at the liquid-air interface, producing streaming flows around the microbubbles that can drive fluid flow. Tovar et al. [112] developed a microbubble pump based on lateral air cavities. By changing the cavity orientation, activation frequency and driving amplitude, the pumping fluids rate reached 250 nL min^{-1}. Similarly, as shown in Fig. 4a, Ryu et al. [102] presented a microfluidic pump by placing a capillary tube above the oscillating bubble and the flow rate was about 0.6 μL s^{-1}. Recently, Gao et al. [114] developed a bidirectional micropump based on the resonant frequency discrepancy for different microbubbles. By tuning the size and location of bubbles, the flow direction can be changed by modifying acoustic frequencies. Moreover, it is also capable of pumping high-viscosity fluids, such as blood-mimicking fluid, without damaging cell fluid delivery.

Besides the bubble-based acoustofluidic pump, vibrating sharp structures can also be adopted to pump fluid by taking advantage of acoustic streaming flows around the structures. For example, in Fig. 4b, Huang et al. [103] realized a programmable acoustofluidic pump utilizing tilted sharp-edge structures. By tuning the input voltage and structure parameter, it was capable of generating flow rate ranging from ~ 10 nL min^{-1} to ~ 100 μL min^{-1}. To provide more tunability and flexibility, Durrer et al. [104] demonstrated a simple and versatile fluid pumping method based on robot-assisted acoustically activated capillaries (Fig. 4c). By positioning the oscillating capillary tip closer to one side of the channel wall, the device generates acoustic streaming vortices and control liquid pumping in a spiral fluidic channel.

The other type of acoustic fluid control is controllable droplet generation. For instance, Zhang et al. [117] proposed a droplet aspirator that utilizes the small radiation pressures with orbit angular momentum induced by a spiral-electrode transducer to produce droplets ranging from micrometer to nanometer scales. To broaden the selection of materials, Foresti et al. [105] took use of an acoustic Fabry-Perot resonator to generate and pattern droplets with various materials, including those with viscosity as high as 25,000 Pa·s (Fig. 4d). In addition to the aforementioned devices that rely on acoustic radiation force, Xu et al. [118] introduced piezoelectric actuators to control the deformation of microchannels, which could produce droplets ranging from 40 pL to 4.5 nL (Fig. 4e). Furthermore, as shown in Fig. 4f, He et al. [106] presented a vibrating sharp-tip capillary which could induce acoustic streaming in the oil phase to generate water droplet with high throughput (up to 5000 droplets s^{-1}). The size of droplet can be controlled (6.77–661 μm) by

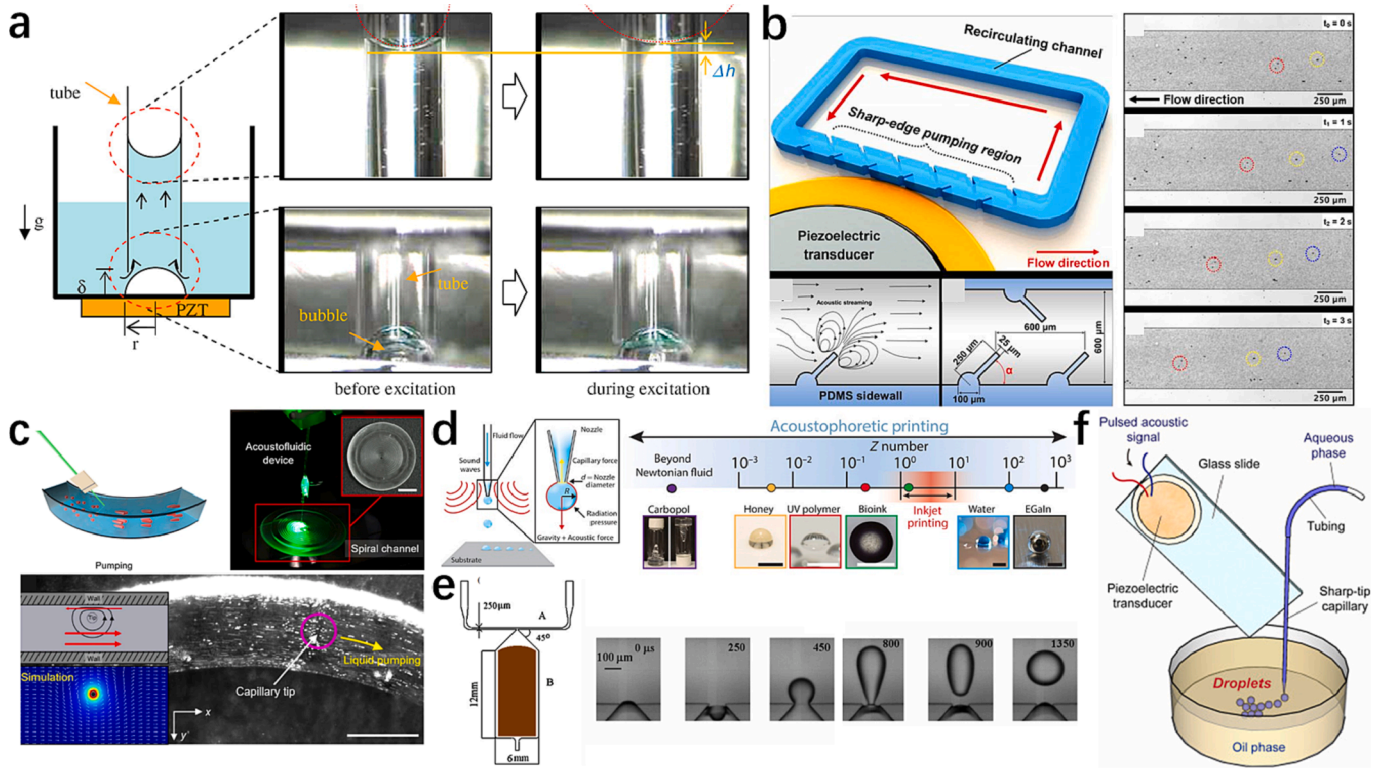

Fig. 4. Acoustofluidic devices for pumping and droplet generation. (a) A microbubble pump based on the oscillating bubble. Reproduced from reference [102]. Copyright 2010, Elsevier B.V. (b) A programmable acoustofluidic pump based on tilted sharp-edge structures. Reproduced from reference [103]. Copyright 2014, Royal Society of Chemistry. (c) Based on the robot-assisted acoustically activated capillary, the produced acoustic streaming vortices can achieve liquid pumping in a spiral fluidic channel. Reproduced from reference [104]. Copyright 2022, Springer Nature Limited. (d) An acoustic Fabry-Perot resonator to generate and pattern droplets with various materials. Reproduced from reference [105]. Copyright 2018, American Association for the Advancement of Science. (e) A droplet generator based on piezoelectric actuators controlled microchannels deformation. Reproduced from reference [118]. Copyright 2008, IOP Publishing. (f) A high throughput droplet generator based on the vibrating sharp-tip capillary induces acoustic streaming in the oil phase. Reproduced from reference [106]. Copyright 2021, Elsevier B.V.

adjusting the acoustic excitation time.

These above studies demonstrate that the implementation of acoustically activated sharp-edge structures and microbubbles can effectively pump fluid and generate droplets. Ultrasound's biocompatibility and good transmission through tissue allow it to induce motion in hard-to-access regions, making it a promising technology for biomedical applications in smart devices.

3.3. Separation and enrichment

Microparticle separation and enrichment have been playing an essential role in biomedical analysis and early disease detection [124,125]. Accurate and rapid diagnosis of certain diseases rely on identifying the associated pathogens or cells. Hence, it becomes imperative to separate these particles for detection and treatment. For example, the separation of circulating tumor cells (CTCs) from human blood cells is quite essential for inchoate diagnosis of cancer. In another example, the separation of platelets from whole blood will greatly contribute to clinical application, as platelets are a rich source of growth factors that can accelerate the recovery of bone and soft tissues. Microfluidics has gained popularity as a method that enables several microscale particle manipulations, applying force gradients on the scale of cells within minute volumes of fluid. These manipulation can be achieved through hydrodynamic techniques [126] or through external energy-based microfluidic devices (e.g., electrical [127], magnetic [128], optical [129] and acoustic [130,131] fields). Among these techniques, acoustofluidic devices are a prospective method for cell separation and enrichment because of their noninvasive, good penetrability and label-free properties [132-134]. In addition, the use of sub-MHz acoustic wavelengths in the medium facilitates particle separation and enrichment as they match the common dimensions of microfluidic channels or chambers.

Acoustic radiation force [119] and acoustic streaming [120,121,135,136] are the two basic mechanisms for microparticle separation. For instance, as shown in Fig. 5a, Chen et al. [119] demonstrated an acoustofluidic device to separate platelets from whole blood. The separation principle is due to the significant difference in acoustic radiation force between the red/white blood cells and the platelets. The device showed high platelet recovery (>85%) and red/white blood cell removal (>80%) at a flow rate of 10 mL min^{-1}. Qiu et al.[137] uses an ultrasonic concentrated energy transducer (UCET) coupled with PDMS channel to separate circulating tumor cells (CTCs) from whole blood. The UCET can generate acoustic radiation force (ARF) for sorting at 20 kHz frequency and the PDMS channel generated inertial forces can be used for pre-focus.

Additionally, microstructures have been designed to separate micro-objects [120,135,136]. Through vibrating these structures, the acoustic streaming flow will be generated around them. Tumor cells [120,135,136] can thus be separated using these methods due to the density and size discrepancy with other cells (Fig. 5b). Furthermore, Garg et al. [121] presented a device for whole-blood separation by lateral cavity acoustic transducers (LCATs). The LCATs function by trapping bubbles in patterned dead-end side channels, creating liquid–gas interfaces that serve as sources of acoustic microstreaming (Fig. 5c).

The sub-MHz acoustic microsystem can also be used to enrich micro/nanoparticles for biomedical and biochemical systems. As presented in Fig. 5d, Xie et al. [53] proposed a bubble-based particle enrichment

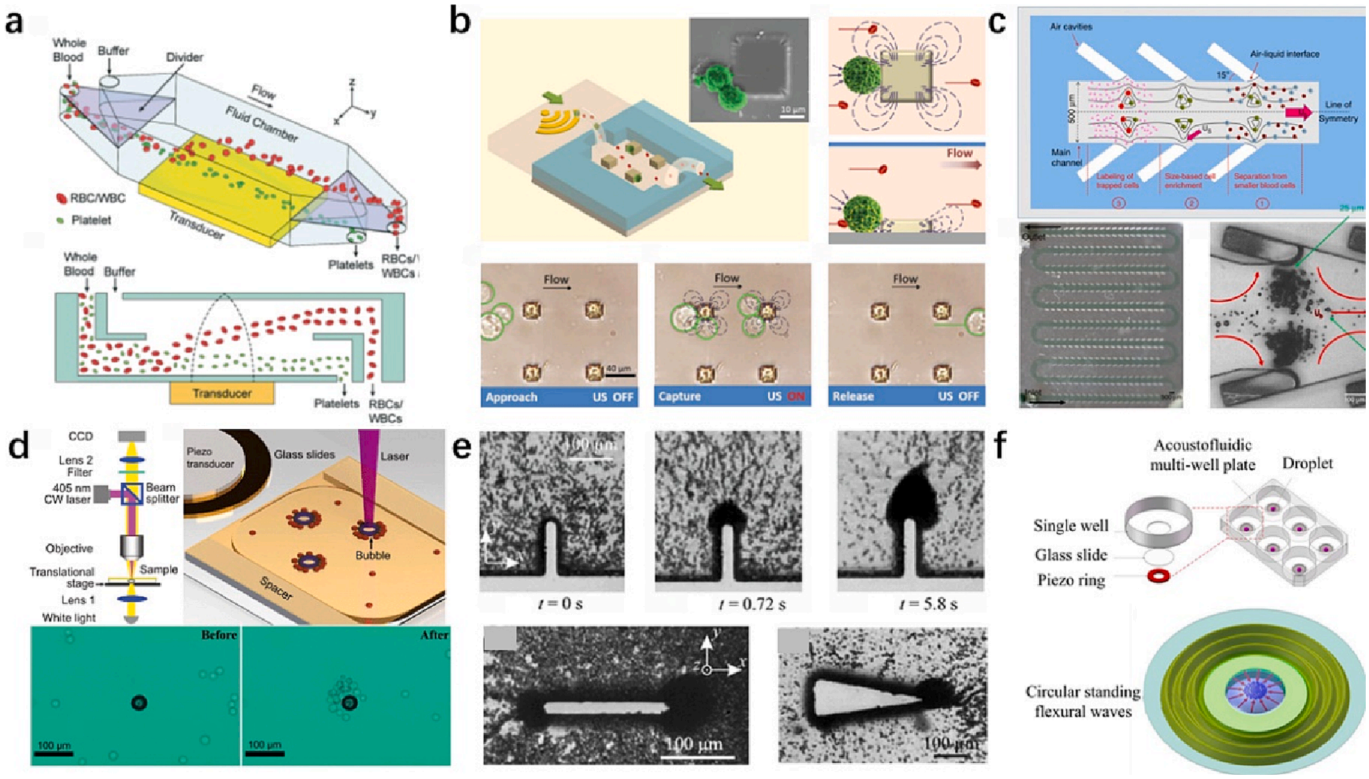

Fig. 5. Acoustofluidic devices for particle separation and enrichment. (a) High-throughput separation of red blood cells/white blood cells and platelets from whole blood using vertical acoustic radiation force difference. Reproduced from reference [119]. Copyright 2016, Royal Society of Chemistry. (b) An acoustic microfluidic trap array to separate cancer cells. Reproduced from reference [120]. Copyright 2019, John Wiley & Sons, Inc. (c) A device for whole blood separation by lateral cavity acoustic transducers (LCATs). Reproduced from reference [121]. Copyright 2018, Elsevier B.V. (d) A technique utilizes the opto-thermal effect to generate bubbles in a microchamber and acoustic radiation force to trap particles/cells. Reproduced from reference [53]. Copyright 2013, Royal Society of Chemistry. (e) Particles enrichment in oscillating sharp edges. Reproduced from reference [122]. Copyright 2015, Springer Nature Limited. (f) Micro/nanoparticles and cells are concentrated in multi-well plates by using a piezo ring array. Reproduced from reference [123]. Copyright 2020, Royal Society of Chemistry.

device. This method employs the laser optothermal effect to generate bubbles, which are subsequently excited using acoustic waves. The resulting acoustic radiation force effectively trapped particles/cells, including 15 μm polystyrene beads and HeLa cells. Zhou et al.[223] explore that ultralow frequency (800Hz) acoustic vibration can effectively concentrate submicron particles at two sides of a micropillar in a microfluidic device. This phenomenon is resulting from a collective effect of acoustic streaming induced drag force and non-Newtonian fluid induced elastic lift force. This means acoustic wave with a wavelength six orders of magnitude larger than the particle size can be used to manipulate particles. Leibacher et al. [122] presented a strategy that utilize vibrating sharp edges induced streaming to trap yeast cells around the sharp edges (Fig. 5e). Similarly, Qi et al. [138] developed a nanoparticle enrichment device, which relies on the acoustic streaming generated by an ultrasonically vibrating micro-manipulated probe inserted into a nanoparticle suspension droplet. More recently, Liu et al. [123] simplified systems by using a piezo ring array to concentrate micro/nanoparticles and cells in multi-well plates, as depicted in Fig. 5f. In this work, the piezoelectric transducer could generate circular standing flexural waves in the substrate of each well. The resulting vibrations caused acoustic streaming near the interface between the substrate and fluid droplet positioned in the well, ultimately leading to the concentration of micro/nanoscale objects at the center of the droplet for enrichment.

These above studies summarized different methods and mechanisms of the sub-MHz acoustic micromanipulation for particle separation and enrichment. Typically, these methods depend on differences in particle size. For particles with similar sizes, acoustofluidic separation methods based on other properties such as impedance and density differences have shown feasibility and great potential. Despite being contactless, biocompatible and noninvasive, it is crucial to separate targets directly from raw samples. Currently, the separation demonstrations still require the usage of pretreated samples.

3.4. Patterning

In the past decades, numerous manipulation approaches have been described in the field of particle assembly and biomedical engineering, especially for cell patterning and tissue regeneration [139-142]. Compared to other techniques, acoustic manipulation shows the advantages of contactless, fast, controllable and spatially precise assembly. Especially, the acoustic manipulation of cells in culture medium, including the collagen solution [143,144], hydrogel [145,146] and other viscous mediums, makes it possible to mimic the dense tissue structure and natural multilayered structure, in which the cells were firstly patterned by acoustic techniques and followed by the cross-linking of the culture medium. Moreover, complex three-dimension (3D) structures can be obtained when applying proper building elements in patterning. For example, 3D organoids can be patterned using spheroids, cell carriers as building elements [147-149]. In this session, we focus on the recent advancements in microparticle patterning based on sub-MHz acoustic systems. The sub-MHz acoustic wave is proven easier to be produced by low-cost acoustic devices compared to the high-frequency wave, and it is capable of presenting a more spatially uniform energy field for particle assembly since larger wavelength in liquid (>1 mm) can better match microchannel or chambers. Generally, according to the different wave types, these works are categorized as flexural wave, Faraday wave and reflective standing wave. These three methods

respectively correspond to the three system setup shown in the general introduction (Fig. 2). In the principle of most patterning methods via sub-MHz acoustic wave, the particles will move to and then be restricted in the position of pressure nodes or antinodes induced by the acoustic wave, of which the phase and amplitude have been usually spatially modulated in the manipulation system.

Faraday wave is the waveform at the liquid–air interface while the liquid bottom is actuated by vertical vibration. Taking the advantage of its complex geometries, which can be tuned by altering the vibration parameters, chamber shape or liquid properties, Faraday wave can pattern the microparticles to diverse structures. Briefly, recirculating flow resulting from Faraday-wave-induced liquid surface deformation will drive the suspended particles to the static positions which are located beneath wave nodes via Stokes drag force, and patterned construction consequently forms.

Demirci et al. reported an acoustic patterning method using Faraday wave to establish the liquid surface morphology for the microscale assembly of floaters [148]. In their work, low-frequency reflective standing wave, no >200 Hz, created diverse liquid-based templates via changing the geometries of the chamber or vibrational parameters, and drift energy gradient was distributed in the liquid surface where the floaters were able to move from low drift energy region to high drift energy region. Their liquid-based template method was available for various materials, including hydrogel, elastomer particles, cell microcarriers and cell spheroids, meanwhile the particles with sizes in the range from 10 μm to 2 mm could be patterned. Using their method, ring-shaped, "H"-shaped, cruciate, stripe-shaped and other combined structure was successfully obtained, as shown in Fig. 6a. The versatility of the Faraday wave has made it attractive in particle patterning and verified the possibility to develop various complex structures.

Furthermore, patterning of cell spheroids or cell-containing elements via Faraday wave has gradually emerged and has been applied to the bio-assembly of the organoid. In 2015, in the same group, Demiric et al. investigated the hepatic organoid assembly by patterning multiple types of cell spheroids with a Faraday wave at a low frequency (120–140 Hz) [147]. They successfully applied acoustic nodes to pattern the fibroblast and endothelial cell spheroids into a ring-shaped structure, which completely fused after 72 h culture to generate vasculature-like constructs. And they further patterned the mixture of hepatocyte spheroids, fibroblast spheroids and endothelial cell spheroids to assemble liver

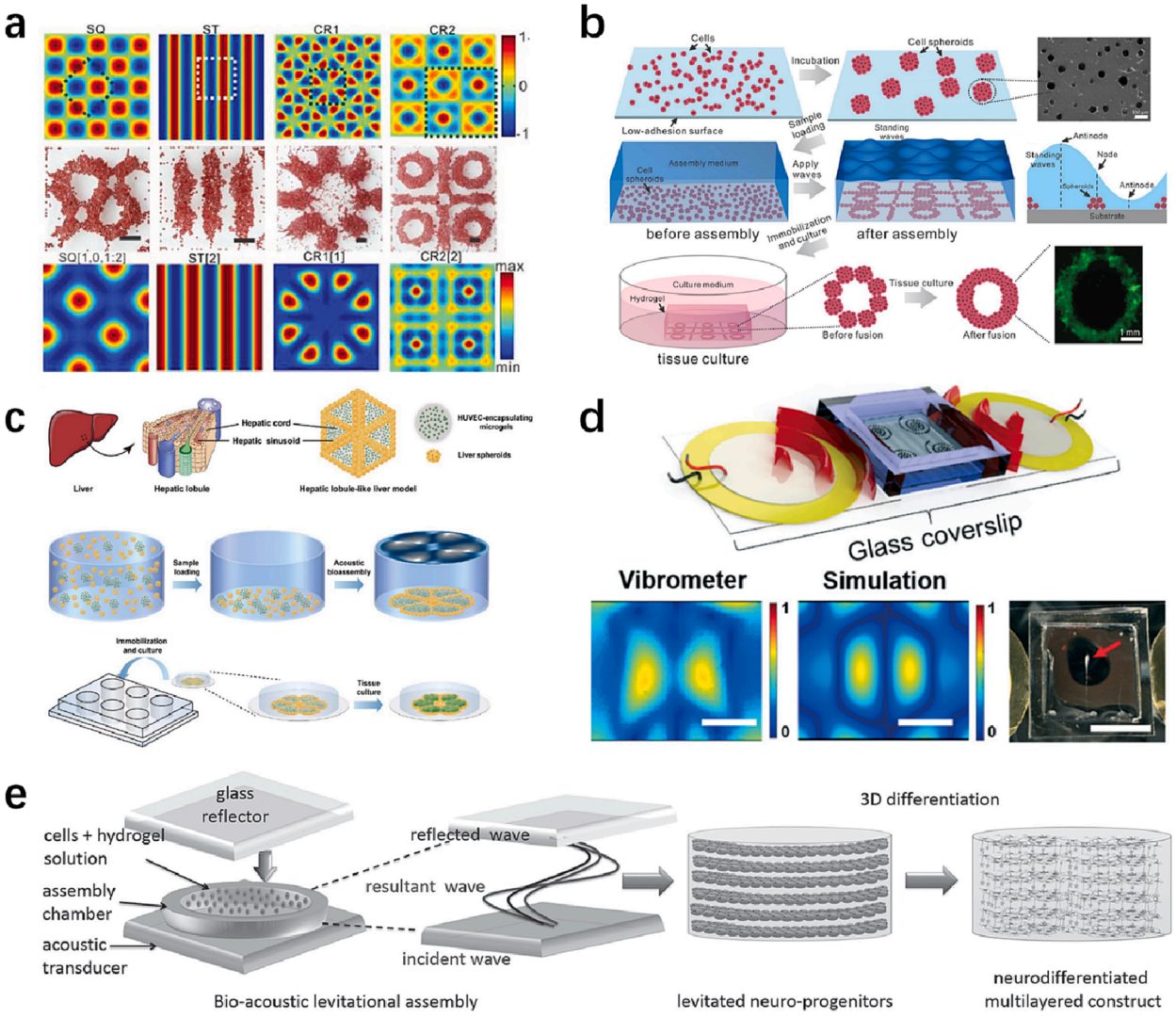

Fig. 6. Sub-MHz acoustic patterning via different types of waves. (a) Liquid-based template generated by Faraday wave for particle patterning. Reproduced from reference [148]. Copyright 2014, John Wiley & Sons, Inc. (b) Schematics of ring-shaped hepatic organoids bio-assembly with Faraday wave. Reproduced from reference [147]. Copyright 2015, John Wiley & Sons, Inc. (c) Patterning of the lobule-like liver model by applying Faraday wave to different heterogeneous cell-containing blocks. Reproduced from reference [149]. Copyright 2022, IOP Publishing. (d) Schematic of the flexural-wave-based device and line-shaped acoustic pressure generation for particle patterning. Reproduced from reference [150]. Copyright 2020, Royal Society of Chemistry. (e) Illustration of Bio-Acoustic Levitational (BAL) device based on plane standing wave for multilayered structure patterning. Reproduced from reference [151]. Copyright 2016, John Wiley & Sons, Inc.

organoids with dense tissue structure after 6-day cell culture, as illustrated in Fig. 6b. More recently, a work co-led by Demiric and Chen showed the differentially bioassembled heterocellular architecture could be constructed by applying the Faraday wave to the mixture of liver spheroids and endothelial cell-encapsulating microgels (Fig. 6c) [149]. Based on size difference and buoyant density difference of cellular building blocks, the bioassembly was capable of forming complementary or sandwich cytoarchitectures beneath nodes (or antinodes) of Faraday wave, resulting in the lobule-like liver model generation, and such spatially defined hepatic lobule model exhibited several liver-related metabolic functions. Their methods provided strategies for organoids formation using acoustic patterning, which may potentially promote the development of tissue engineering and regenerative medicine.

Faraday wave can also be applied for the bioassembly of microscale objectives smaller than cells to generate microorganism-based biostructure. Hong and his colleagues recently presented a fascinating work to control the formation of biofilms with a 45–120 Hz Faraday wave which was excited by different vertical accelerations [152]. They kept the thickness of the liquid layer in the microplate wells at 2 mm and applied a Faraday wave to persuade the motion of *E. coli* (*Escherichia coli*) on the well bottom, which finally developed into ring-shaped, flower-shaped or unstable square-shaped biofilms according to different vibration accelerations. In their work, the bacteria were driven to the antinodes of the surface wave after 24-hour stimulation, indicating the feasibility of acoustic manipulation for bioassembly within a long duration.

Flexural waves, another low-frequency wave that can induce wall-liquid boundary deformation in the direction perpendicular to their propagation, have also been explored for particle patterning. Similarly, flexural waves achieve patterning by trapping particles in pressure nodes along the vibrating substrate, and the manipulation of particles is usually operated in an open well. In a work presented by Bachman et al., they mounted two bilateral piezoelectric transducers and a middle PDMS well on a glass substrate to form an acousticfluidic device based on the flexural wave [150]. Applying the signals with a frequency of 4.8 kHz out of phase to excite two transducers, they found two antinodes with a middle line-shaped low pressure were generated in the well (Fig. 6d), which could be used to pattern the particles into a line. Aghakhani and colleagues also reported the particle trapping method using a flexural-wave-based acoustic system comprised of a single piezoelectric transducer and PDMS channel on a glass substrate [153]. By increasing the wavelength-to-channel width ratio, higher radiation force would be induced, which contributed to the wall-trapping effect of the particles. Flexural waves have been gradually applied to particle patterns in the open chamber since their generation are independent of the chamber shape, and the low frequency of flexural waves makes it possible to manipulate the particle on a larger wall surface [150].

Similarly, the principle of patterning by the reflective standing wave is trapping particles into nodes or antinodes to consequently form the interested spatial distribution of particles, whereas the patterning using reflective standing wave is conducted in a closed chamber. Demirci et al. developed a Bio-Acoustic Levitational (BAL) device to create 3D multilayer tissue of neuro-progenitor cells (NPCs), mimicking the physiological characteristic of the native cerebral cortex [151]. Their BAL device for standing wave generation involved a ceramic acoustic generator, a glass reflector and an acrylic levitation chamber, as shown in Fig. 6e. In their work, the reflective standing wave induced parallel node planes to levitate NPCs that dispersed in fibrin solution within seconds by acoustic radiation force, followed by fibrin cross-linking to form 3D multilayer constructs. And the interlayer distance could be altered by changing the frequency of the reflective standing wave, which aided to match the natural spacing of the layer structure of the cerebral cortex. The patterning via the nodes and antinodes plane induced by a reflective standing wave can be considered as a sophisticated approach for multilayered structure formation, and the complexity of spatial distribution of the nodes (antinodes), to a great extent, determined the configuration of patterned construction.

Utilization of the Bjerknes force is also an additional approach to achieving particle patterning. Radaud et al. patterned the bubbles (20–50 μm) in microchannel as 'crystal-like' lattices with side affixed transducer frequency of 155 kHz [46]. In their design, the distance between each gathering bubble could be tuned through input frequency, which determined the magnitude of Bjerknes force applied to a certain bubble from its neighbouring bubble. Those work deftly exploited Bjerknes force between bubbles to perform patterning, showing the potential to create microarchitectures with the utilization of secondary acoustic radiation force.

More and more acoustic methods have been gradually investigated to pattern the particles into the personalized structure. The particles within the liquid can be assembled into specific patterns within seconds when using the acoustic wave, which is a fast and efficient process. Since acoustic patterning is contactless, rapid, adjustable and biocompatible, those impressive approaches show the versatility of acoustic wave in particle assembly and exhibit their potential in biomanufacturing, especially for tissue engineering and regenerative medicine.

3.5. Rotation

The rotational manipulation of micro-objects can assist the multi-angle imaging of structures and features. The rotated micro-objects of rotation include cells, embryos, seeds etc. Rotating these objects can achieve all-around observation, characterization analysis, label-free sorting, and biomarker detection. Conventional methods, such as micropipes or microneedles, commonly require direct contact with the microparticles which may cause damage to the bio-sample. Acoustic-based rotation manipulation has recently emerged as a promising method for rotating microparticles, particularly in biological samples. This technique can achieve non-contact rotating microparticles, thus decreasing damage. Additionally, the rotatable micro-objects have a wide size range from several nanometers to several millimetres. In comparison to the high-frequency acoustic rotation [154], the sub-MHz acoustic devices have a larger acoustic wavelength, thus providing a more homogeneous acoustic field to drive the micro-rotation. Moreover, the sub-MHz microsystems are based on more accessible acoustic components such as buzzers, and piezoelectric plates, dispense with the microfabrication procedures, which are advantageous for its mass production.

The rotation method can be classified into two main categories: in-plane rotation and out-of-plane rotation. The plane is the one that is parallel with the observing camera plane. In-plane rotation means the micro-object rotates parallel to the observing camera plane. Out-of-plane rotation indicates that the micro-object can rotate not only parallel to the observing plane. Both rotation control in the sub-MHz acoustic microsystem can integrate with other manipulation easily, like mixing [159] and patterning [160]. For example, Ozcelik et al. [155] demonstrated the acoustic rotation of organisms in a guided wave propagation setup. The acoustic wave at 1–100 kHz range was generated from a buzzer and transmitted via the glass substrate to excite the resonance of sharp-edge structures. Due to the acoustic streaming effect, the vibrating microstructure induced microstreaming to trap and rotate the single cell (~20 μm). The streaming-induced flow by microchannel could even manipulate the rotation of single particle length up to 1000 μm elegans (Fig. 7a). Feng et al. [161] also achieved single oocyte multiplane rotation manipulation using similar microfluidic devices.

The vibrating direction of the microstructure is an essential factor for the sub-MHz acoustic rotation system, as the different vibration directions lead to different acoustic streaming profiles. To precisely control it, Hayakawa et al. [156] utilized a three-dimensional vibration stage, which contains three individual actuation respectively along X/Y/Z directions. The stage vibrated at a low frequency of 100–200 Hz and drove the microstructures to vibrate in the same manner. The directed

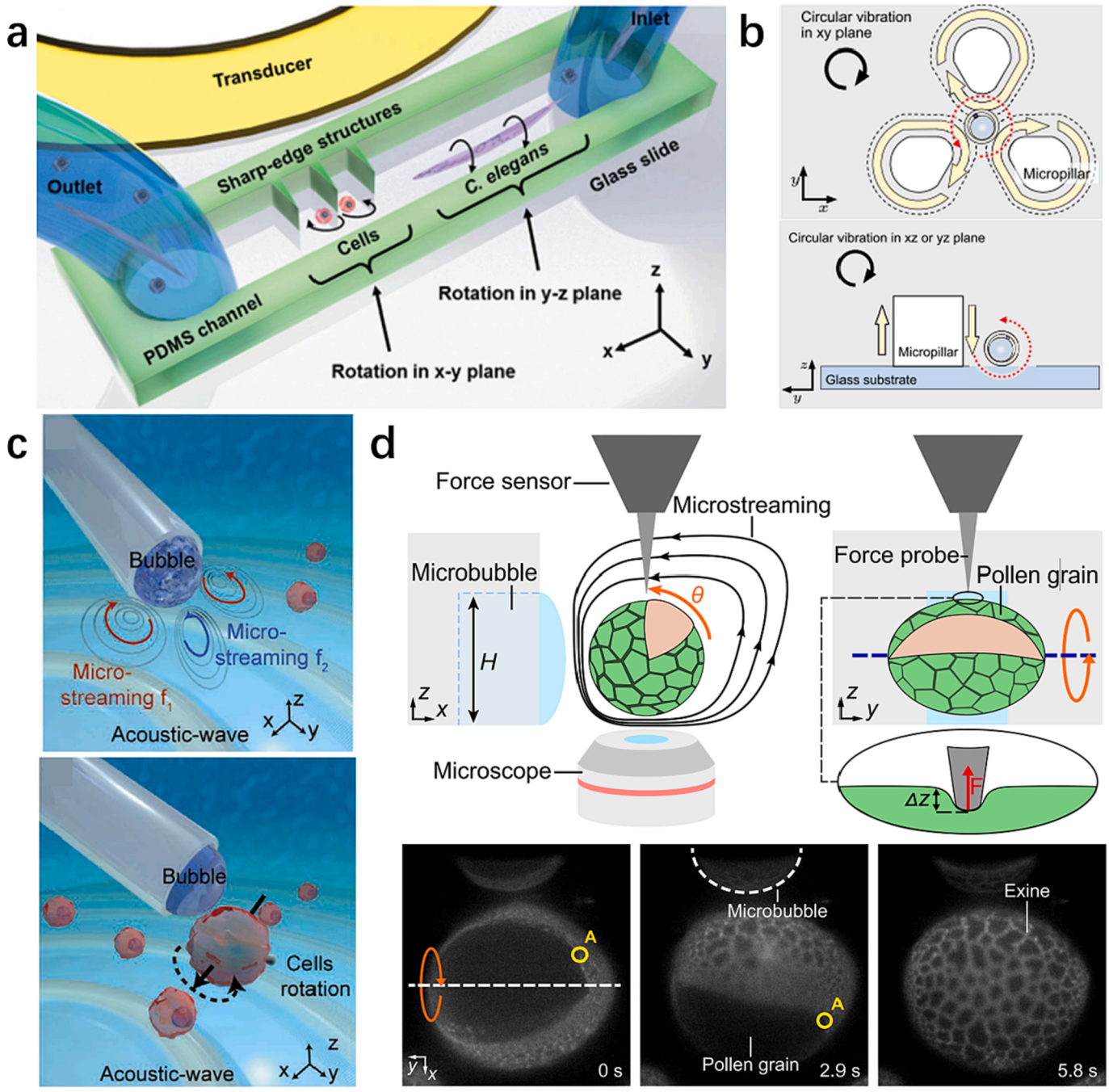

Fig. 7. Microparticle rotation in a sub-MHz acoustic microsystem. (a) Schematic and the working principle of the acoustic rotation system. A microchannel contains both sharp-edge and bare regions for cell rotation. Oscillations of the sharp-edge microstructures and the glass slide generate circulating streaming flows that are used for rotational manipulation. Reproduced from reference [155]. Copyright 2016, John Wiley & Sons, Inc. (b) Oocyte 3D rotation based on vibration-induced local whirling flow. A pillar array placed on bulk vibration stage can also supply applications for particle transportation, gathering, trapping and rotation. Reproduced from reference [156]. Copyright 2015, Springer Nature Limited. (c) The microbubble vibrates in an acoustic field to generate acoustic streaming flows, which trap and rotate the cells. Reproduced from reference [157]. Copyright 2021, John Wiley & Sons, Inc. (d) Acoustic streaming, generated by the resonant vibration of microbubbles, traps and re-orients the pollen grains with respect to the force sensor, which enables the 3D mechanical characterization of it. Reproduced from reference [158]. Copyright 2021, Springer Nature Limited.

vibration of the microstructures generated a flow to trap and rotate the mouse oocyte (~50 μm) along different planes. As shown in Fig. 7b, when circular vibration along the X-Y plane was applied to a microchip with micropillar patterns, the cell was in-plane rotated; while the stage vibration was applied with Z-components, the cell was out-of-plane rotated. Thus, the direction and velocity of this flow can be controlled by changing the direction and amplitude of the stage vibration. The same group also explored various pillar forms' influence on pillar-around flow and possible applications [162]. Taking advantage of precise control over the vibration direction, Liu et al. demonstrated the needle-guided circular vibration driven by the piezoelectric stage could rotate cells or cell spheroids. [163].

Similar to the vibrating microstructure, the vibration of the liquid–air interface also generates acoustic streaming for rotating the micro-objects. In the sub-MHz acoustic frequency range, the microbubbles usually have multiple resonant frequencies, thus correspondingly

generating diverse streaming profiles [164-166]. Based on this mechanism, Zhou et al. [157] show that a soft-contact acoustic microgripper with a bubble generated at the tip of the microcapillary can capture, transport and rotate microbeads (20–65 μm) and zebrafish (950 μm-1.4 mm) by coupled radiation force and drag force on the microparticles, enabling multimode movements and keep bioparticles activity (Fig. 7c). By out-of-plane rotating the biosample, mechanical characterization of Lilium Longiflorum pollen grains and Caenorhabditis elegans nematodes using acoustic rotation and force microscopy were conducted (Fig. 7d) [158]. It reveals local variations in apparent stiffness for micro-living systems and may be used as the basis for biophysical modelling.

3.6. Propulsion and actuation

Contactless propulsion and actuation of micro-object, known as micropropeller or microswimmer, have been extensively studied in the recent decade, which have great potential applications in biomedical research [167,168]. Acoustic methods for micro-object propulsion and actuation commonly rely on the vibration of sharp-edge structures or microbubbles to induce streaming for propulsive force. These methods have favorable safety, biocompatibility and simple system setup. Such advantages provide huge benefits to be applied in biomedical scenarios [40].

With the development of micro-manufacturing technology, complex structures with a specific character (bubble [178], sharp edge [179]) can be designed and fabricated as micropropeller. For example, Kaynak et al. [169] fabricated a bio-inspired sperm-like micropropeller, which was propelled by flagellum-induced microstreaming. The linear velocity has reached 1200 μm s^{-1} (Fig. 8a). Dillinger et al. [170] developed ultrasound-activated synthetic ciliary bands inspired by the natural ciliary arrangements on the surface of starfish larvae. The liquid flow controlled by ciliary bands can be used for propulsion (Fig. 8b). Bertin et al. [171] designed armored microbubbles which allowed the bubbles to last for hours even under forced oscillations. Net propulsive flow generated by the bubble vibration could reach 100 mm s^{-1} in 320 kHz (Fig. 8c). Lu et al. [180] also presented a superfast strategy for growing dandelion-like micro swarms from tubular micromotors and driving them to move freely with an average speed of up to 50 mm s^{-1} in 101 kHz by oscillating self-generated bubbles in an ultrasound field.

The control of micropropeller is an important issue in the way of their wide applications. One method is based on resonance frequency changes with the bubble size thus bubble can be actuated selectively. While different-sized bubbles are placed in different positions of the micropropeller, turning control can be realized by activating the bubble independently [178,181]. Qiu et al. [182] showed highly directional propulsion could be generated from active acoustic surfaces that consisted of two-dimension (2D) arrays of microcavities holding microbubbles and turned centimeter-scale devices in water selectively. Luo et al.[172] designed a two-bubble micropropeller with different opening diameters. The micropropeller could swim in a straight line at 301 kHz frequency and turned to rotate at 234 kHz frequency, as shown in Fig. 8d.

Some researchers investigated the combination of the magnetic/electric/chemical and acoustic fields for manipulating micropropeller. For example, Aghakhani et al. [173] presented bullet-shaped micropropellers coated anisotropically with a soft magnetic nanofilm layer, allowing steering under a magnetic field. Interestingly, they performed either the straight moving trajectory or turning events with 90 degrees upon the magnetic field functioned, shown in Fig. 8e. They also accomplished high shear rate propulsion of acoustic microrobots in complex biological fluids (non-Newtonian fluids) by the same micropropeller and control method [183]. A similar approach also can be achieved at higher frequency (≥1 MHz) [184]. In another study, Bai et al. [185] presented that a magnetized macrophage robot could target and kill cancer cells using a combination of external acoustic and magnetic fields. Gao et al.[186] take advantage of the self-spinning of microsphere in 100 ~ 200 kHz ultrasound. In which spinning is attributed to localized, circular streaming flow around microsphere. Then acoustic spinning was used to steer surface catalysis powered micromotor and AC electric field powered micromotor, respectively. An example of approach, pick up, transport and release cargos are demonstrated. Overall, the combination of acoustic propulsion and other power field (magnetic, electric and chemical) steering can be effectively utilized to actuate and navigate micropropeller in confined and hard-to-reach body location areas in a minimally invasive fashion.

As above, acoustic streaming is considered as a major method of directional transport at small scales. Researchers have also investigated other acoustic mechanical effects. Arora et al. [174,187] also observed corrugated, hydrophilic microparticles causing cavitation inception at their surface when they were exposed to a strong tensile stress wave. The growing cavity thus accelerated the particle into translatory motion, and speed reached ~ 40 m s^{-1}. When the volume growth of the cavity slowed down, the particle detached from the cavity through a process of neck-breaking, and the particle was shot away (Fig. 8f).

In contrast to an untethered micropropeller, acoustic propulsion is also used to generate torque for micromechanical systems. The commonly used sharp edge [175,188] and bubble [189,190] structures are introduced into the rotor arm or by assembling micropropellers in a spinner structure, the rotor can be actuated at high speed within acoustic field [171,188]. Zhou et al. [175] achieved the uniform actuation of multiple microrotors with high rotational speed by a piezoelectric vibration stage (see Fig. 8g). The paired asymmetric acoustic streaming generated by a series of curved sharp tips on the microrotor produces a net torque to propel rotor rotation. The microrotor rotational speed could be controlled through rotor arm numbers and input frequency, which achieved the rotational speed of ~ 1600 RPM at the piezoelectric vibration stage and oscillated at only 800 Hz. Except for the rotor, many devices which need spin movement may be achieved by acoustic actuation. Qiu et al. [191] reported the miniaturization of a urological endoscope by acoustic actuation. The thin-layer surface actuator is based on two-dimensional arrays of microbubbles that resonance with external ultrasound, giving rise to frequency-selective acoustic streaming thus achieving wireless control and multiple freedom degrees. It shows the potential medical applicability of acoustic microrotor. Another interesting study was that Kaynak et al. [176] designed an acoustically excited μjet engine fabricated by 3D printing. The pumping was generated by the tip of the conical wedge-induced acoustic streaming, as shown in Fig. 8h. Various monolithic compound micromachinery with multiple engines function to collect, encapsulate, and process microscopic samples.

Except for micropropeller and microrotor, structure-vibrating induced streaming is also an actuation method for the surrounding microparticles. For particle manipulation with a complex path, Lu et al. [177] proposed a new approach that achieved the directional particle/cell movement inside the pre-defined complex maze at the side affixed transducer frequency of 134 kHz, which was relying on the acoustically induced localized microstreaming generated around microstructures, as shown in Fig. 8i. Using the same local microstreaming in sub-MHz frequency, they proposed a controllable high-speed acoustic rotary microsystem that particle rotated along a micropillar [192] and a method that assembled microparticles to a straight chain at the pillar's narrow opening end [193]. They also developed the platform for microparticle accurate movement upon input signal [194] and vision feedback control [195]. Ahmed et al. [196] also showed bio-inspired rolling motion by introducing superparamagnetic particles in magnetic and acoustic fields, inspired by a neutrophil rolling on a wall. The particles can self-assemble due to dipole–dipole interaction in the presence of a rotating magnetic field. The aggregate migrates towards the wall of the channel due to the radiation force of an acoustic field. Structure-vibrating actuation will benefit targeted therapeutics and non-invasive surgery, especially for the need with precise motion in the vasculature.

In conclusion, the main advantage of propulsion using an acoustic

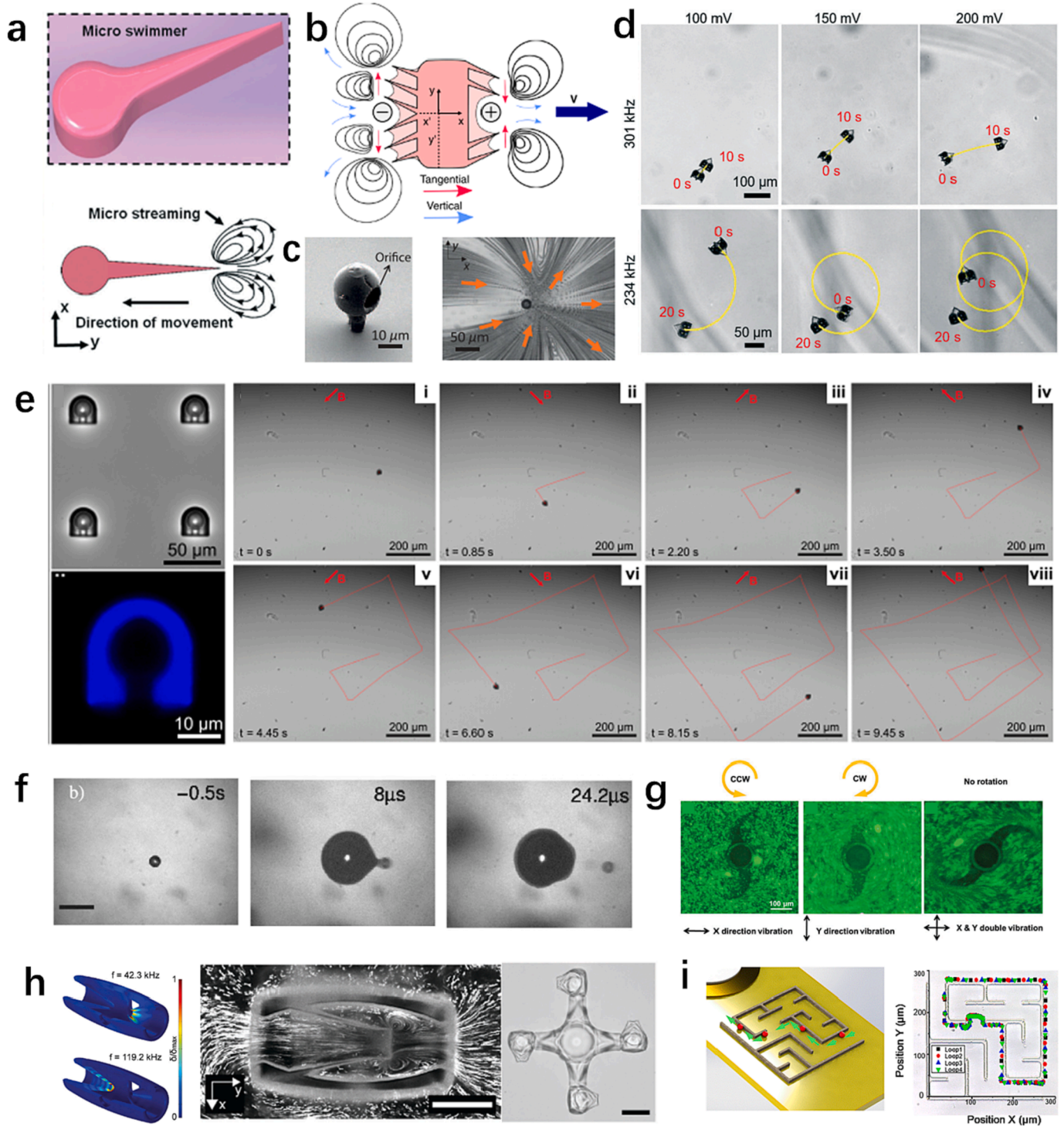

Fig. 8. Micro-object propulsion and actuation in sub-MHz acoustic microsystems. (a) Schematic of bio-inspired sperm-like micropropeller, which is propelled by acoustic streaming effect. Reproduced from reference [169]. Copyright 2017, Royal Society of Chemistry. (b) Starfish larva-inspired synthetic ciliary band design for micropropeller. The synthetic cilia can be acoustically actuated to drive bulk fluid motion. Reproduced from reference [170]. Copyright 2021, Springer Nature Limited. (c) An armored microbubbles micropropeller (size range, 10–20 μm) made by three-dimensional microfabrication. Reproduced from reference [171]. Copyright 2015, American Physical Society. (d) A two-bubble-based micropropeller with different opening diameters in which the bubble can be selectively actuated for motion control. Reproduced from reference [172]. Copyright 2021, Royal Society of Chemistry. (e) A bullet-shaped micropropeller that can be acoustically actuated and magnetically steered. Reproduced from reference [173]. Copyright 2020, National Academy of Science. (f) The process of growing a cavity on the surface of corrugated, hydrophilic microparticles actuates the particle. When the cavity growth slows down, the particle detaches from the cavity and shot away. Reproduced from reference [174]. Copyright 2004, American Physical Society. (g) Uniform actuation of multiple microrotors with high rotational speed by a piezoelectric vibration stage. Reproduced from reference [175]. Copyright 2020, John Wiley & Sons, Inc. (h) An acoustically excited μjet engine fabricated by 3D printing. The pumping is generated by the tip of the conical wedge-induced acoustic streaming. Reproduced from reference [176]. Copyright 2020, John Wiley & Sons, Inc. (i) The directional particle/cell movement inside the pre-defined complex maze under structure-vibrating induced streaming. Reproduced from reference [177]. Copyright 2017, American Chemical Society.

field is its ability to relatively accurate and contactless control. Additionally, swarm control can be achieved in a large-scale area in sub-MHz frequency. Finally, broad adaptability in arbitrary solutions of the acoustic propulsion device provides a great prospect for practical biomedical applications.

3.7. Other applications

Besides the basic acoustic micromanipulation listed in sessions 3.1–3.6, some other applications especially in the biological field are introduced in this session. The first one is cell lysis with sub-MHz acoustic waves. Cell lysis is a critical step for bio-detection and diagnosis applications due to the highly valuable biomolecules such as proteins, DNA and RNA, as well as disease biomarkers enclosed within the cell membrane. By acoustically oscillating sharp edges [202] or microbubbles [197], acoustic streaming is locally generated and derived shear forces that can physically rupture cell membranes. Existing research have shown continuous and >90% lysis efficiency , as seen in Fig. 9a. Malaria is a life-threating disease caused by parasites, which plagues a significant population of the world. Thus, better diagnostic platforms are necessary for enhancing detection sensitivity, whilst reducing processing times, sample volumes and cost. One critical process is the effective lysis of blood samples. Amir et al. [198]designed a star shaped acoustofluidic mixer for enhanced blood cell lysis. the device is capable of lysing a 20 × dilution of isolated red blood cells (RBCs) with an efficiency of ~95% within 350 ms (0.1 mL). (Fig. 9b).

Cell sonoporation is another application that employs cavitation bubbles to generate transient pores in the cell membrane [203,204], then foreign substances can enter cells easily by passing through the pores, which provides promising prospects for drug delivery [205] and gene transfection [206]. In fact, there are a number of studies on sonoporation but in high frequency(>1MHz). For example, Connor et al. [207] developed a spiral microfluidic channel based microfluidic device. The ultrasound probe as the acoustic source induces microbubble rupture under 2.5 MHz, leading to transient perforation of cell membranes—enabling enhanced intracellular delivery of soluble compounds such as trehalose. Meng et al.[208] shown that 24 MHz surface acoustic wave generated by IDTs can be used to induce microbubble destruction at the desired location and achieve targeted cell sonoporation. Nevertheless, sonoporation effect under sub-MHz frequency still have some applications. As presented in Fig. 9c, microbubble arrays and sharp edge arrays are commonly adopted to trap cells and transiently modulate the permeability of cell membrane for homogenous sonoporation at single cell level [199,209]. Michael et al. [210] found that low- frequency (250 kHz) insonation of microbubbles results in high amplitude oscillation in vitro that increase the uptake of large molecules. Alinaghi et al. [211] present a sonoporation strategy for adherent cells at 96 kHz frequency. Mechanical oscillation propagated by guided wave facilitates the cellular uptake of different size cargo materials through endocytic. The dosage of delivered cargo can be controlled by actuation voltage

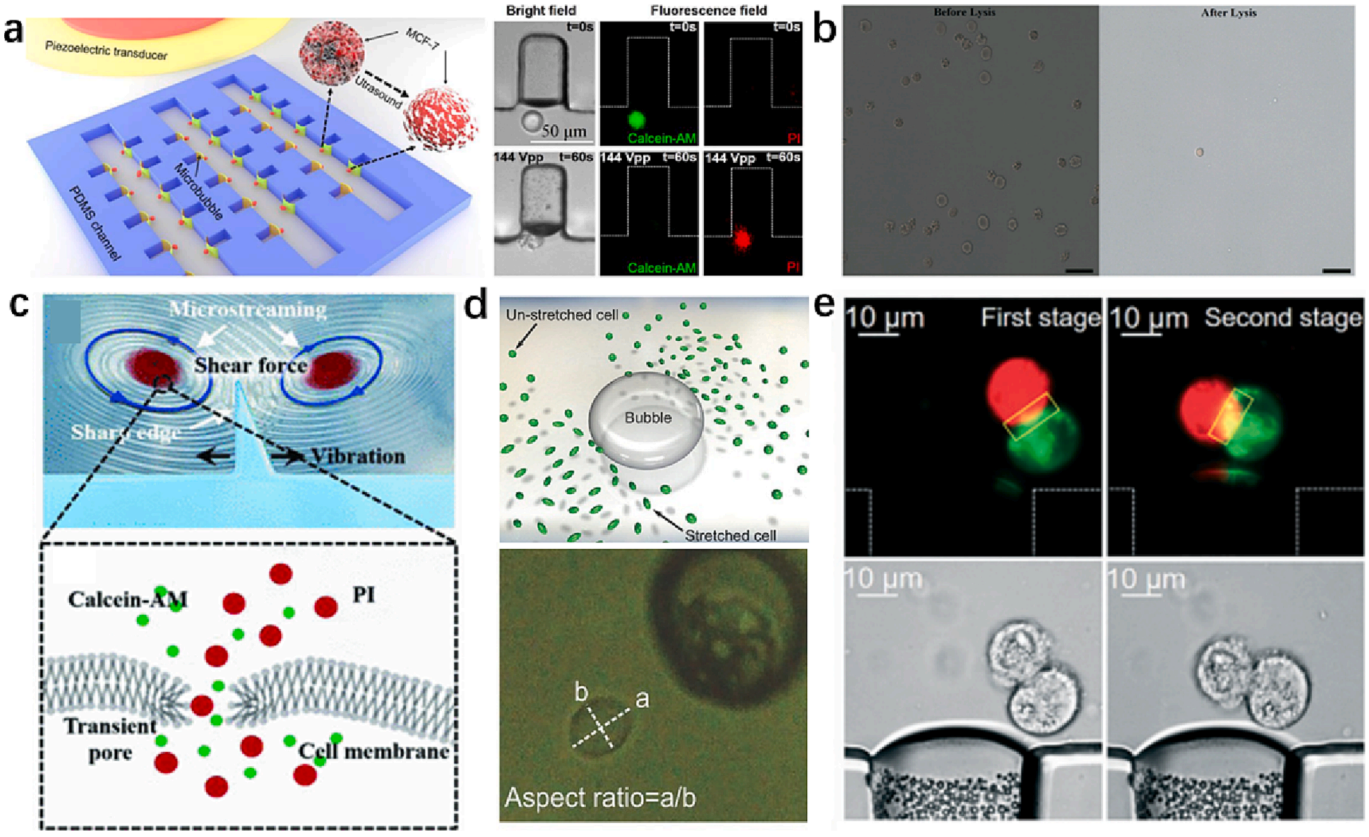

Fig. 9. Other applications in a sub-MHz acoustic microsystem. (a) Schematic of MCF-7 cell lysis. A single cell in the vicinity of the air bubble. As the MCF-7 cell membrane is intact, the green fluorescence generated by the living cells is observed. After the ultrasound irradiation, the MCF-7 cell is broken into pieces, and only the red fluorescence is observed. Reproduced from reference [197]. Copyright 2020, Published by MDPI. (b) Microscope imaging of RBCs samples before and after lysis. Reproduced from reference [198]. Copyright 2022, Royal Society of Chemistry. (c) Microstreaming formed to generate high shear forces for cell trapping and sonoporation. The schematic of the sonoporation events, indicating Calcein-AM and PI can pass through the cell membrane via the transient pore. Reproduced from reference [199]. Copyright 2020, IEEE. (d) schematic for cell stretching in the flow field around an acoustically activated oscillating bubble; a spherical-shaped suspended cell is stretched near an oscillating bubble, where the aspect ratio is used to characterize the cell's deformability. Reproduced from reference [200]. Copyright 2016, John Wiley & Sons, Inc. (e) Process of heterotypic membrane cell fusion. Fluorescent and bright images for MCF-7 cell (red color) and MDA-MB-231 cell (green color) membrane fusion. Reproduced from reference [201]. Copyright 2022, Royal Society of Chemistry.

and treatment duration. Song et al. [212] applied acoustically vaporized nanodroplets to enhance the transmembrane permeability effect for opening the blood–brain-barrier (BBB). The detailed sonoporation mechanism can be seen in the review [213]. Cell deformation (Fig. 9d) also can be realized by acoustic-induced streaming for distinguishing their mechanical properties [200]. Cell fusion (Fig. 9e) is an essential event in many biological processes and has been demonstrated that cell capture, pairing, and fusion are based on oscillating bubbles within an acoustofluidic device [201]. In short, sub-MHz acoustic micromanipulation plays an extremely crucial role in point-of-care technologies and is attracting more research attentions [4].

4. Conclusion and perspective

As discussed above, interest in the sub-MHz acoustic wave-based microfluidic particle manipulation has increased in the last few years. The different microparticle handling methods have enabled diverse applications in biomedicine. We briefly introduce the basic mechanisms that appeared in sub-MHz acoustic particle manipulation, including acoustic radiation force, acoustic streaming and acoustic cavitation. The setup is classified by the wave propagation method as guided wave propagation, transmissive wave propagation and standing wave. The diverse manipulations, including mixing, pumping and droplet generation, separation and enrichment, patterning, rotation, propulsion and actuation are reviewed.

The adaptability of applications with a such wide range is based on the following advantages: (1) particle manipulation with a size range from submicron to millimeter scale; (2) low requirement on particle and liquid parameters, such as magnetic labelling, electrical conductivity, etc.; (3) great biocompatibility with minimum harm on biological samples; (4) a wide range of throughput handling from nanoliter to milliliter; (5) last but not least, for the sub-MHz frequency range, low cost due to the simple setup and acoustic source requirement (buzzer, speaker, or piezoelectric plate). These advantages make the techniques easier to be promoted as large-scale applications and commercialization.

Aiming at further improvements on the sub-MHz acoustic micromanipulation, the following aspects should be concerned and explored:

1. The acoustic manipulation devices have multiple functions as shown in session 3. However, most existing manipulating systems are demonstrated with one basic function or deal with a single biochemical process. This makes it hard to afford the whole analysis process from sample preparation to the final test. Integrating various functions into one system can expand their universality. With systematic integration, a series of portable, multi-function, user-friendly biomedical analysis systems can be expected.
2. Owing to the complexity of fluid mechanics, further deeply theoretical exploration (such as analytical solution) on bulk vibration induced outer boundary layer streaming needs to be conducted, which can provide precise description and optimize the guidance upon particle manipulation microfluidic device design.
3. Although the resolution of sub-MHz acoustic wave-based microfluidic particle manipulation can reach submicron and realize high throughput handling, it is not suitable for applications with extremely high requirements on manipulation resolution (<100 nm) due to its inherent frequency settings (typically kHz to a few MHz). In such cases, researchers may opt for the surface acoustic wave platform actuated by high frequency IDTs (hundreds of MHz to GHz), offering high accuracy and high resolution but requiring compromise on the low volume sample handling. Thus, combination of sub-MHz acoustic wave-based methods with high throughput and surface acoustic wave platform exhibiting high resolution can perform the potential solution.
4. Current research breakthroughs are typically limited in the in vitro systems. For in vivo applications, the sub-MHz acoustic micromanipulation has several potential research directions. Across-tissue manipulation based on sub-MHz acoustic waves is suitable for in vivo applications, which means acoustic sources can remotely actuate the micro-objects. In addition to quality and safety, biocompatibility is also of particular importance. Some applications are more applicable in vivo, like Gao et al. [214] showed ultrasound thrombolysis using acoustic bubbles in vitro. By combining the acoustic field with the optical or magnetic field, the development of on-chip micro-robotics with biocompatible materials will greatly promote the application of minimally invasive medicine in the clinical field.
5. The precision of the present manipulation method also requires further improvement, such as rotation and prolusion. One of the potential directions is to add feedback control, which may benefit auto and accurate manipulation for circumventing personal error. However, proper and matched observation methods require further investigation, such as ultrasound imaging, magnetic resonance imaging, etc.
6. To some extent, there are still a lot of applications in the field of applied acoustics, especially sonochemistry, which have not been studied in a precise or controllable microfluidic system. For example, viscosity variations of heavy crude oil [215], ultrasound-assisted water purification [216], quick freezing [217], air drying [218], protein modification [219], etc. While these techniques have been utilized extensively in industry, the challenge of implementing that into microfluidic devices still exists. It may be possible to adapt these methods currently used to manipulate microparticles in the microchip, thus developing new manage methods to expand application scenes of acoustic manipulation devices. There has been a batch of hopeful works about the sub-MHz frequency acoustic which have been performed to date and their capabilities need to be investigated by future experimental work.
7. Though sub-MHz acoustic micromanipulation has been applied in cells and tissues, the influence of acoustic streaming/cavitation effect for bionic samples are not clear enough in microfluid devices. Several studies about ultrasonic and tissue engineering/cell have been reported [220,221]. For example, Guo et al. [222] apply low intensity pulse ultrasound (LIPUS) to improve the porosity and permeability of a 3-D alginate scaffold, thus benefiting nutrition supply and metabolism during cell growth. The physics mechanism might lie in microstreaming shear stress generated by ultrasound-driven microbubble oscillations. However, excessively delivered acoustic energy might cause undesired cell damage. Thus, evaluation of the interaction between sub-MHz acoustic and bionic samples is worthy to explore, which has profound significance for biological application.

Looking into the future, micromanipulation has been identified as a major bottleneck to advancing the biomedical and environmental fields. The sub-MHz acoustic wave-based manipulation exhibits good biocompatibility, low cost, and simple setup, which are promising in enhancing future biochemical analysis and benefit healthcare.

CRediT authorship contribution statement

Yu Liu: Writing – original draft. **Qiu Yin:** Writing – original draft. **Yucheng Luo:** Writing – original draft. **Ziyu Huang:** Writing – review & editing. **Quansheng Cheng:** Writing – review & editing. **Wenming Zhang:** Writing – review & editing. **Yinning Zhou:** Conceptualization, Writing – review & editing, Supervision. **Zhichao Ma:** Conceptualization, Writing – review & editing, Supervision.

Declaration of Competing Interest

The authors declare that they have no known competing financial interests or personal relationships that could have appeared to influence the work reported in this paper.

Data availability

Data will be made available on request.

Acknowledgments

The work is supported by National Natural Science Foundation of China (Grant No. 12032015), the Innovation Program of Shanghai Municipal Education Commission (Grant No. 2019-01-07-00-02-E00030), Shanghai Pilot Program for Basic Research Shanghai Jiao Tong University (Grant No. 21TQ1400203), The Science and Technology Development Fund, Macau SAR (0021/2022/A1, 006/2022/ALC), and Research Grant (MYRG2022-00088-IAPME, SRG2021-00003-IAPME) from the Research & Development Administration Office at the University of Macau.

References

[1] P. Li, T.J. Huang, Applications of acoustofluidics in bioanalytical chemistry, Anal. Chem. 91 (2019) 757–767.
[2] A. Ozcelik, J. Rufo, F. Guo, Y. Gu, P. Li, J. Lata, T.J. Huang, Acoustic tweezers for the life sciences, Nat. Methods 15 (2018) 1021–1028.
[3] M. Wiklund, R. Green, M. Ohlin, Acoustofluidics 14: Applications of acoustic streaming in microfluidic devices, Lab Chip 12 (2012) 2438–2451.
[4] Y. Xie, H. Bachman, T.J. Huang, Acoustofluidic methods in cell analysis, TrAC Trends Anal. Chem. 117 (2019) 280–290.
[5] W. Connacher, N. Zhang, A. Huang, J. Mei, S. Zhang, T. Gopesh, J. Friend, Micro/nano acoustofluidics: materials, phenomena, design, devices, and applications, Lab Chip 18 (2018) 1952–1996.
[6] M. Baudoin, J.-L. Thomas, Acoustic tweezers for particle and fluid micromanipulation, Annu. Rev. Fluid Mech. 52 (2020) 205–234.
[7] J. Jalal, T.S.H. Leong, Microstreaming and its role in applications: A mini-review, Fluids 3 (2018) 93.
[8] A. Lenshof, C. Magnusson, T. Laurell, Acoustofluidics 8: Applications of acoustophoresis in continuous flow microsystems, Lab Chip 12 (2012) 1210–1223.
[9] V. Marx, Biophysics: using sound to move cells, Nat. Methods 12 (2015) 41–44.
[10] L.Y. Yeo, J.R. Friend, Surface acoustic wave microfluidics, Annu. Rev. Fluid Mech. 46 (2014) 379–406.
[11] G. Destgeer, H.J. Sung, Recent advances in microfluidic actuation and micro-object manipulation via surface acoustic waves, Lab Chip 15 (2015) 2722–2738.
[12] L. Meng, F. Cai, F. Li, W. Zhou, L. Niu, H. Zheng, Acoustic tweezers, J. Phys. D Appl. Phys. 52 (2019), 273001.
[13] J. Friend, L.Y. Yeo, Microscale acoustofluidics: Microfluidics driven via acoustics and ultrasonics, Rev. Mod. Phys. 83 (2011) 647–704.
[14] P. Zhang, H. Bachman, A. Ozcelik, T.J. Huang, Acoustic microfluidics, Annu. Rev. Anal. Chem. 13 (2020) 17–43.
[15] Z. Chen, X. Liu, M. Kojima, Q. Huang, T. Arai, Advances in micromanipulation actuated by vibration-induced acoustic waves and streaming flow, Appl. Sci. 10 (2020) 1260.
[16] J.G. Kralj, M.T.W. Lis, M.A. Schmidt, K.F. Jensen, Continuous dielectrophoretic size-based particle sorting, Anal. Chem. 78 (14) (2006) 5019–5025.
[17] J. Voldman, Electrical forces for microscale cell manipulation, Annu. Rev. Biomed. Eng. 8 (1) (2006) 425–454.
[18] S. Park, M. Koklu, A. Beskok, Particle trapping in high-conductivity media with electrothermally enhanced negative dielectrophoresis, Anal. Chem. 81 (6) (2009) 2303–2310.
[19] D.R. Link, E. Grasland-Mongrain, A. Duri, F. Sarrazin, Z. Cheng, G. Cristobal, M. Marquez, D.A. Weitz, Electric control of droplets in microfluidic devices, Angew. Chem. Int. Ed. 45 (16) (2006) 2556–2560.
[20] J. Kim, J.H. Shin, Stable, Free-space optical trapping and manipulation of sub-micron particles in an integrated microfluidic chip, Sci. Rep. 6 (2016) 33842.
[21] Y. Zhang, Y. Li, Y. Zhang, C. Hu, Z. Liu, X. Yang, J. Zhang, J. Yang, L. Yuan, HACF-based optical tweezers available for living cells manipulating and sterile transporting, Opt. Commun. 427 (2018) 563–566.
[22] X. Wang, S. Chen, M. Kong, Z. Wang, K.D. Costa, R.A. Li, D. Sun, Enhanced cell sorting and manipulation with combined optical tweezer and microfluidic chip technologies, Lab Chip 11 (2011) 3656–3662.
[23] M. Hejazian, W. Li, N.T. Nguyen, Lab on a chip for continuous-flow magnetic cell separation, Lab Chip 15 (2015) 959–970.
[24] C. Murray, E. Pao, P. Tseng, S. Aftab, R. Kulkarni, M. Rettig, D. Di Carlo, Quantitative magnetic separation of particles and cells using gradient magnetic ratcheting, Small 12 (2016) 1891–1899.
[25] A. Fakhfouri, C. Devendran, A. Ahmed, J. Soria, A. Neild, The size dependant behaviour of particles driven by a travelling surface acoustic wave (TSAW), Lab Chip 18 (2018) 3926–3938.
[26] F. Petersson, L. Aberg, A.M. Sward-Nilsson, T. Laurell, Free flow acoustophoresis: microfluidic-based mode of particle and cell separation, Anal. Chem. 79 (2007) 5117–5123.
[27] D.J. Collins, Z. Ma, J. Han, Y. Ai, Continuous micro-vortex-based nanoparticle manipulation via focused surface acoustic waves, Lab Chip 17 (2016) 91–103.
[28] K. Zhang, Y. Ren, M. Zhao, T. Jiang, L. Hou, H. Jiang, Flexible microswimmer manipulation in multiple microfluidic systems utilizing thermal buoyancy-capillary convection, Anal. Chem. 93 (2021) 2560–2569.
[29] H. Cong, J. Chen, H.-P. Ho, Trapping, sorting and transferring of micro-particles and live cells using electric current-induced thermal tweezers, Sens. Actuators B Chem. 264 (2018) 224–233.
[30] W.-Z. Fang, T. Xiong, O.S. Pak, L. Zhu, Data-driven intelligent manipulation of particles in microfluidics, Adv. Sci. 10 (5) (2023) 2205382.
[31] M. Tanyeri, M. Ranka, N. Sittipolkul, C.M. Schroeder, A microfluidic-based hydrodynamic trap: design and implementation, Lab Chip 11 (2011) 1786–1794.
[32] Y. Zhou, Z. Ma, Y.e. Ai, Hybrid microfluidic sorting of rare cells based on high throughput inertial focusing and high accuracy acoustic manipulation, RSC Adv. 9 (53) (2019) 31186–31195.
[33] J. Gao, M.L. Sin, T. Liu, V. Gau, J.C. Liao, P.K. Wong, Hybrid electrokinetic manipulation in high-conductivity media, Lab Chip 11 (2011) 1770–1775.
[34] J. Rufo, P. Zhang, R. Zhong, L.P. Lee, T.J. Huang, A sound approach to advancing healthcare systems: the future of biomedical acoustics, Nat. Commun. 13 (2022) 3459.
[35] J. Rufo, F. Cai, J. Friend, M. Wiklund, T.J. Huang, Acoustofluidics for biomedical applications, Nat. Rev. Methods Primers 2 (2022).
[36] S. Zhao, D. Sun, J. Zhang, H. Lu, Y. Wang, R. Xiong, K.T.V. Grattan, Actuation and biomedical development of micro-/nanorobots – A review, Mater. Today Nano 18 (2022), 100223.
[37] K. Kolesnik, M. Xu, P.V. Lee, V. Rajagopal, D.J. Collins, Unconventional acoustic approaches for localized and designed micromanipulation, Lab Chip 21 (2021) 2837–2856.
[38] Y. Li, X. Liu, Q. Huang, A.T. Ohta, T. Arai, Bubbles in microfluidics: an all-purpose tool for micromanipulation, Lab Chip 21 (2021) 1016–1035.
[39] J. Rufo, F. Cai, J. Friend, M. Wiklund, T.J. Huang, Acoustofluidics for biomedical applications, Nat. Rev. Methods Primers 2 (2022) 30.
[40] J. Li, C.C. Mayorga-Martinez, C.-D. Ohl, M. Pumera, Ultrasonically propelled micro- and nanorobots, Adv. Funct. Mater. 32 (5) (2022) 2102265.
[41] D. Ahmed, X. Mao, J. Shi, B.K. Juluri, T.J. Huang, A millisecond micromixer via single-bubble-based acoustic streaming, Lab Chip 9 (2009) 2738–2741.
[42] L. Brillouin, R.O. Brennan, Tensors in mechanics and elasticity, J. Appl. Mech. 32 (1965), 238-238.
[43] L.P. Gor'kov, On the forces acting on a small particle in an acoustical field in an ideal fluid, Solviet Physics Doklady (1962) 773.
[44] T. Laurell, F. Petersson, A. Nilsson, Chip integrated strategies for acoustic separation and manipulation of cells and particles, Chem. Soc. Rev. 36 (3) (2007) 492–506.
[45] V. Bjerknes, Fields of Force: Supplementary Lectures, Applications to Meteorology; a Course of Lectures in Mathematical Physics Delivered December 1 to 23, 1905, Columbia University Press, 1906.
[46] D. Rabaud, P. Thibault, M. Mathieu, P. Marmottant, Acoustically bound microfluidic bubble crystals, Phys. Rev. Lett. 106 (2011), 134501.
[47] S.J. Lighthill, Acoustic streaming, J. Sound Vib. 61 (1978) 391–418.
[48] C. Eckart, Vortices and streams caused by sound waves, Phys. Rev. 73 (1948) 68–76.
[49] H. Schlichting, Berechnung ebener periodischer Grenzschichtstromungen, Phys. Z. 33 (1932) 327–335.
[50] J.W. Strutt, I., On the circulation of air observed in Kundt's tubes, and on some allied acoustical problems, Philos. Trans. R. Soc. Lond. 175 (1884) 1–21.
[51] T.G. Leighton, 2 - Cavitation Inception and Fluid Dynamics, in: T.G. Leighton (Ed.), The Acoustic Bubble, Academic Press, 1994, pp. 67–128.
[52] C.C. Church, E.L. Carstensen, "Stable" inertial cavitation, Ultrasound Med. Biol. 27 (2001) 1435–1437.
[53] Y. Xie, C. Zhao, Y. Zhao, S. Li, J. Rufo, S. Yang, F. Guo, T.J. Huang, Optoacoustic tweezers: a programmable, localized cell concentrator based on opto-thermally generated, acoustically activated, surface bubbles, Lab Chip 13 (2013) 1772–1779.
[54] A. Iranzo, F. Chauvet, Synthesis of in situ purified iron nanoparticles in an electrochemical and vibrating microreactor: study of ramified branch fragmentation by oscillating bubbles, Microfluid. Nanofluid. 23 (2019).
[55] X. Lu, Y. Wei, H. Ou, C. Zhao, L. Shi, W. Liu, Universal control for micromotor swarms with a hybrid sonoelectrode, Small 17 (2021) e2104516.
[56] S. Orbay, A. Ozcelik, J. Lata, M. Kaynak, M. Wu, T.J. Huang, Mixing high-viscosity fluids via acoustically driven bubbles, J. Micromech. Microeng. 27 (1) (2017) 015008.
[57] T. Leighton, The principles of cavitation, Ultrasound Food Process. 12 (1998).
[58] J.R. Lindner, Contrast echocardiography, Curr. Probl. Cardiol. 27 (2002) 454–519.
[59] A.G. Athanassiadis, Z. Ma, N. Moreno-Gomez, K. Melde, E. Choi, R. Goyal, P. Fischer, Ultrasound-responsive systems as components for smart materials, Chem. Rev. 122 (2022) 5165–5208.
[60] N.H. An Le, H. Deng, C. Devendran, N. Akhtar, X. Ma, C. Pouton, H.K. Chan, A. Neild, T. Alan, Ultrafast star-shaped acoustic micromixer for high throughput nanoparticle synthesis, Lab Chip 20 (2020) 582–591.
[61] V.C. Patel, W. Rodi, G. Scheuerer, Turbulence models for near-wall and low Reynolds number flows-a review, AIAA J. 23 (9) (1985) 1308–1319.
[62] K.S. Ryu, K. Shaikh, E. Goluch, Z. Fan, C. Liu, Micro magnetic stir-bar mixer integrated with parylene microfluidic channels, Lab Chip 4 (2004) 608–613.
[63] A.N. Hellman, K.R. Rau, H.H. Yoon, S. Bae, J.F. Palmer, K.S. Phillips, N. L. Allbritton, V. Venugopalan, Laser-induced mixing in microfluidic channels, Anal. Chem. 79 (12) (2007) 4484–4492.

[64] C.-Y. Lee, C.-L. Chang, Y.-N. Wang, L.-M. Fu, Microfluidic mixing: a review, Int. J. Mol. Sci. 12 (2011) 3263–3287.
[65] A. Jahn, S.M. Stavis, J.S. Hong, W.N. Vreeland, D.L. DeVoe, M. Gaitan, Microfluidic mixing and the formation of nanoscale lipid vesicles, ACS Nano 4 (4) (2010) 2077–2087.
[66] J.-C. Hsu, C.-Y. Chang, Enhanced acoustofluidic mixing in a semicircular microchannel using plate mode coupling in a surface acoustic wave device, Sens. Actuators, A 336 (2022) 113401.
[67] Z. Chen, Z. Pei, X. Zhao, J. Zhang, J. Wei, N. Hao, Acoustic microreactors for chemical engineering, Chem. Eng. J. (Lausanne) 433 (2022) 133258.
[68] D. Ahmed, X. Mao, B.K. Juluri, T.J. Huang, A fast microfluidic mixer based on acoustically driven sidewall-trapped microbubbles, Microfluid. Nanofluid. 7 (5) (2009) 727–731.
[69] D. Ahmed, C.Y. Chan, S.-C. Lin, H.S. Muddana, N. Nama, S.J. Benkovic, T. Jun Huang, Tunable, pulsatile chemical gradient generation via acoustically driven oscillating bubbles, Lab Chip 13 (3) (2013) 328–331.
[70] K.Y. Lee, S. Park, Y.R. Lee, S.K. Chung, Magnetic droplet microfluidic system incorporated with acoustic excitation for mixing enhancement, Sens. Actuators, A 243 (2016) 59–65.
[71] S. Zhao, C. Yao, Q. Zhang, G. Chen, Q. Yuan, Acoustic cavitation and ultrasound-assisted nitration process in ultrasonic microreactors: The effects of channel dimension, solvent properties and temperature, Chem. Eng. J. 374 (2019) 68–78.
[72] Y. Gao, P. Tran, K. Petkovic-Duran, T. Swallow, Y. Zhu, Acoustic micromixing increases antibody-antigen binding in immunoassays, Biomed. Microdevices 17 (2015) 79.
[73] Z. Yang, S. Matsumoto, H. Goto, M. Matsumoto, R. Maeda, Ultrasonic micromixer for microfluidic systems, Sens. Actuators, A 93 (2001) 266–272.
[74] A. Neild, T.W. Ng, G.J. Sheard, M. Powers, S. Oberti, Swirl mixing at microfluidic junctions due to low frequency side channel fluidic perturbations, Sens. Actuators B 150 (2010) 811–818.
[75] S. Orbay, A. Ozcelik, H. Bachman, T.J. Huang, Acoustic actuation of in situ fabricated artificial cilia, J. Micromech. Microeng. 28 (2) (2018) 025012.
[76] P.H. Huang, Y. Xie, D. Ahmed, J. Rufo, N. Nama, Y. Chen, C.Y. Chan, T.J. Huang, An acoustofluidic micromixer based on oscillating sidewall sharp-edges, Lab Chip 13 (2013) 3847–3852.
[77] C. Tian, W. Liu, R. Zhao, T. Li, J. Xu, S.-W. Chen, J. Wang, Acoustofluidics-based enzymatic constant determination by rapid and stable in situ mixing, Sens. Actuators B 272 (2018) 494–501.
[78] H. Bachman, C. Chen, J. Rufo, S. Zhao, S. Yang, Z. Tian, N. Nama, P.H. Huang, T. J. Huang, An acoustofluidic device for efficient mixing over a wide range of flow rates, Lab Chip 20 (2020) 1238–1248.
[79] P. Chen, S. Li, Y. Guo, X. Zeng, B.-F. Liu, A review on microfluidics manipulation of the extracellular chemical microenvironment and its emerging application to cell analysis, Anal. Chim. Acta 1125 (2020) 94–113.
[80] P.H. Huang, C.Y. Chan, P. Li, N. Nama, Y. Xie, C.H. Wei, Y. Chen, D. Ahmed, T. J. Huang, A spatiotemporally controllable chemical gradient generator via acoustically oscillating sharp-edge structures, Lab Chip 15 (2015) 4166–4176.
[81] D. Ahmed, H.S. Muddana, M. Lu, J.B. French, A. Ozcelik, Y. Fang, P.J. Butler, S. J. Benkovic, A. Manz, T.J. Huang, Acoustofluidic chemical waveform generator and switch, Anal. Chem. 86 (2014) 11803–11810.
[82] P.H. Huang, C.Y. Chan, P. Li, Y. Wang, N. Nama, H. Bachman, T.J. Huang, A sharp-edge-based acoustofluidic chemical signal generator, Lab Chip 18 (2018) 1411–1421.
[83] T. Won, D. Jang, K.Y. Lee, S.K. Chung, Acoustic Bubble-Induced Microstreaming for Biochemical Droplet Mixing Enhancement in Electrowetting (EW) Microfluidic Platforms, J. Microelectromech. Syst. 30 (2021) 783–790.
[84] Z. Dong, C. Yao, X. Zhang, J. Xu, G. Chen, Y. Zhao, Q. Yuan, A high-power ultrasonic microreactor and its application in gas-liquid mass transfer intensification, Lab Chip 15 (2015) 1145–1152.
[85] Z. Dong, C. Yao, Y. Zhang, G. Chen, Q. Yuan, J. Xu, Hydrodynamics and mass transfer of oscillating gas-liquid flow in ultrasonic microreactors, AIChE J 62 (2016) 1294–1307.
[86] L. Yang, F. Xu, G. Chen, Enhancement of gas-liquid mass transfer and mixing in zigzag microreactor under ultrasonic oscillation, Chem. Eng. Sci. 247 (2022) 117094.
[87] Q. Zhang, Z. Dong, S. Zhao, Z. Liu, G. Chen, Ultrasound-assisted gas–liquid mass transfer process in microreactors: The influence of surfactant, channel size and ultrasound frequency, Chem. Eng. J. 405 (2021).
[88] S. Zhao, C. Yao, Z. Dong, Y. Liu, G. Chen, Q. Yuan, Intensification of liquid-liquid two-phase mass transfer by oscillating bubbles in ultrasonic microreactor, Chem. Eng. Sci. 186 (2018) 122–134.
[89] S. Zhao, Z. Dong, C. Yao, Z. Wen, G. Chen, Q. Yuan, Liquid-liquid two-phase flow in ultrasonic microreactors: Cavitation, emulsification, and mass transfer enhancement, AIChE J 64 (2018) 1412–1423.
[90] L. Liu, Z. Liu, S. Zhao, C. Yao, G. Chen, The separation and enrichment of molecules with part amphipathy using a novel ultrasonic emulsion-enrichment method, Chem. Eng. J. 444 (2022) 136682.
[91] P.H. Huang, S. Zhao, H. Bachman, N. Nama, Z. Li, C. Chen, S. Yang, M. Wu, S. P. Zhang, T.J. Huang, Acoustofluidic synthesis of particulate nanomaterials, Adv Sci (Weinh) 6 (2019) 1900913.
[92] S. Zhao, P.H. Huang, H. Zhang, J. Rich, H. Bachman, J. Ye, W. Zhang, C. Chen, Z. Xie, Z. Tian, P. Kang, H. Fu, T.J. Huang, Fabrication of tunable, high-molecular-weight polymeric nanoparticles via ultrafast acoustofluidic micromixing, Lab Chip 21 (2021) 2453–2463.
[93] Z. Dong, A.P. Udepurkar, S. Kuhn, Synergistic effects of the alternating application of low and high frequency ultrasound for particle synthesis in microreactors, Ultrason. Sonochem. 60 (2020), 104800.
[94] M.R. Rasouli, M. Tabrizian, An ultra-rapid acoustic micromixer for synthesis of organic nanoparticles, Lab Chip 19 (2019) 3316–3325.
[95] X. Zhao, H. Chen, Y. Xiao, J. Zhang, Y. Qiu, J. Wei, N. Hao, Rational design of robust flower-like sharp-edge acoustic micromixers towards efficient engineering of functional 3D ZnO nanorod array, Chem. Eng. J. 447 (2022) 137547.
[96] N. Hao, P. Liu, H. Bachman, Z. Pei, P. Zhang, J. Rufo, Z. Wang, S. Zhao, T. J. Huang, Acoustofluidics-assisted engineering of multifunctional three-dimensional zinc oxide nanoarrays, ACS Nano 14 (2020) 6150–6163.
[97] Y. Xie, D. Ahmed, M.I. Lapsley, S.C. Lin, A.A. Nawaz, L. Wang, T.J. Huang, Single-shot characterization of enzymatic reaction constants Km and kcat by an acoustic-driven, bubble-based fast micromixer, Anal. Chem. 84 (2012) 7495–7501.
[98] H. Chen, C. Chen, S. Bai, Y. Gao, G. Metcalfe, W. Cheng, Y. Zhu, Multiplexed detection of cancer biomarkers using a microfluidic platform integrating single bead trapping and acoustic mixing techniques, Nanoscale 10 (2018) 20196–20206.
[99] A.J. Conde, I. Keraite, A.E. Ongaro, M. Kersaudy-Kerhoas, Versatile hybrid acoustic micromixer with demonstration of circulating cell-free DNA extraction from sub-ml plasma samples, Lab Chip 20 (2020) 741–748.
[100] S. Zhao, W. He, Z. Ma, P. Liu, P.H. Huang, H. Bachman, L. Wang, S. Yang, Z. Tian, Z. Wang, Y. Gu, Z. Xie, T.J. Huang, On-chip stool liquefaction via acoustofluidics, Lab Chip 19 (2019) 941–947.
[101] P.H. Huang, L. Ren, N. Nama, S. Li, P. Li, X. Yao, R.A. Cuento, C.H. Wei, Y. Chen, Y. Xie, A.A. Nawaz, Y.G. Alevy, M.J. Holtzman, J.P. McCoy, S.J. Levine, T. J. Huang, An acoustofluidic sputum liquefier, Lab Chip 15 (2015) 3125–3131.
[102] K. Ryu, S.K. Chung, S.K. Cho, Micropumping by an acoustically excited oscillating bubble for automated implantable microfluidic devices, J. Assoc. Lab. Autom. 15 (3) (2010) 163–171.
[103] P.H. Huang, N. Nama, Z. Mao, P. Li, J. Rufo, Y. Chen, Y. Xie, C.H. Wei, L. Wang, T. J. Huang, A reliable and programmable acoustofluidic pump powered by oscillating sharp-edge structures, Lab Chip 14 (2014) 4319–4323.
[104] J. Durrer, P. Agrawal, A. Ozgul, S.C.F. Neuhauss, N. Nama, D. Ahmed, A robot-assisted acoustofluidic end effector, Nat. Commun. 13 (2022) 6370.
[105] D. Foresti, K.T. Kroll, R. Amissah, F. Sillani, K.A. Homan, D. Poulikakos, J. A. Lewis, Acoustophoretic printing, Sci. Adv. 4 (8) (2018) e1659.
[106] Z. He, J. Wang, B.J. Fike, X. Li, C. Li, B.L. Mendis, P. Li, A portable droplet generation system for ultra-wide dynamic range digital PCR based on a vibrating sharp-tip capillary, Biosens. Bioelectron. 191 (2021) 113458.
[107] M.Z. Bazant, T.M. Squires, Induced-charge electrokinetic phenomena: theory and microfluidic applications, Phys. Rev. Lett. 92 (2004), 066101.
[108] J. Atencia, D.J. Beebe, Magnetically-driven biomimetic micro pumping using vortices, Lab Chip 4 (2004) 598–602.
[109] J. Leach, H. Mushfique, R. di Leonardo, M. Padgett, J. Cooper, An optically driven pump for microfluidics, Lab Chip 6 (2006) 735–739.
[110] Z. Tan, M. Yang, M. Ripoll, Microfluidic pump driven by anisotropic phoresis, Phys. Rev. Appl 11 (5) (2019) e054004.
[111] Z. Wu, H. Cai, Z. Ao, A. Nunez, H. Liu, M. Bondesson, S. Guo, F. Guo, A digital acoustofluidic pump powered by localized fluid-substrate interactions, Anal. Chem. 91 (11) (2019) 7097–7103.
[112] A.R. Tovar, A.P. Lee, Lateral cavity acoustic transducer, Lab Chip 9 (1) (2009) 41–43.
[113] A.R. Tovar, M.V. Patel, A.P. Lee, Lateral air cavities for microfluidic pumping with the use of acoustic energ, Microfluid. Nanofluid. 10 (2011) 1269–1278.
[114] Y. Gao, M. Wu, Y. Lin, W. Zhao, J. Xu, Jie Xu, Acoustic bubble-based bidirectional micropump, Microfluid. Nanofluid. 24 (4) (2020).
[115] A. Ozcelik, Z. Aslan, A practical microfluidic pump enabled by acoustofluidics and 3D printing, Microfluid Nanofluidics 25 (2021) 5.
[116] P.L. Zhenzhen Chen, X. Zhao, L. Huang, Y. Xiao, Y. Zhang, J. Zhang, Nanjing Hao Sharp-edge acoustic microfluidics: Principles, structures, and applications, Appl. Mater. Today 25 (2021), 101239.
[117] J.Y. Han Zhang, Yun Zhou, Jianfeng Zheng, Yong Cheng, Bichao Bai, Guoxin Zhang, Yisheng Lv, Micro/nanoliter droplet extraction by controlling acoustic vortex with miniwatt, arXiv preprint, (2021).
[118] J. Xu, D. Attinger, Drop on demand in a microfluidic chip, J. Micromech. Microeng. 18 (6) (2008) 065020.
[119] Y. Chen, M. Wu, L. Ren, J. Liu, P.H. Whitley, L. Wang, T.J. Huang, High-throughput acoustic separation of platelets from whole blood, Lab Chip 16 (2016) 3466–3472.
[120] A.M. Xiaolong Lu, Fernando Soto, Pavimol Angsantikul, Jinxing Li, Chuanrui Chen, Yuyan Liang, Hu Junhui, Liangfang Zhang, Joseph Wang, Parallel label-free isolation of cancer cells using arrays of acoustic microstreaming traps, Adv. Mater. Technol. 4 (2019) e1800374.
[121] T.M.W. Neha Garg, V. Liu, R. Liu, E.L. Nelson, A.P. Lee, Whole-blood sorting, enrichment and in situ immunolabeling of cellular subsets using acoustic microstreaming, Microsyst. Nanoeng. 4 (2018) 1–9.
[122] I. Leibacher, P. Hahn, J. Dual, Acoustophoretic cell and particle trapping on microfluidic sharp edges, Microfluid. Nanofluid. 19 (4) (2015) 923–933.
[123] P. Liu, Z. Tian, N. Hao, H. Bachman, P. Zhang, J. Hu, T.J. Huang, Acoustofluidic multi-well plates for enrichment of micro/nano particles and cells, Lab Chip 20 (18) (2020) 3399–3409.
[124] M.A. Witek, I.M. Freed, S.A. Soper, Cell separations and sorting, Anal. Chem. 92 (1) (2020) 105–131.

[125] J. Rufo, F. Cai, J. Friend, M. Wiklund, T.J. Huang, Tony Jun Huang, Acoustofluidics for biomedical applications, Nat. Rev. Methods Primers 2 (1) (2022).
[126] L.J. Kim, C. Wu, et al., Inertial focusing in non-rectangular cross-section microchannels and manipulation of accessible focusing positions, Lab Chip 16 (2016) 992–1001.
[127] S.V. Puttaswamy, P. Xue, Y. Kang, Y. Ai, Simple and low cost integration of highly conductive three-dimensional electrodes in microfluidic devices, Biomed. Microdev. 17 (2015) 4.
[128] Q.-H. Gao, W.-M. Zhang, H.-X. Zou, W.-B. Li, H. Yan, Z.-K. Peng, G. Meng, Label-free manipulation via the magneto-Archimedes effect: fundamentals, methodology and applications, Mater. Horiz. 6 (2019) 1359–1379.
[129] B.H.H. Jin Ho Jung, Oh Yong Suk, Kyung Heon Lee, Kang Soo Lee, Hyung Jin Sung, Optical separation of droplets on a microfluidic platform, Microfluid. Nanofluid. 16 (2014) 635–644.
[130] Z. Wang, H. Wang, R. Becker, J. Rufo, S. Yang, B.E. Mace, M. Wu, J. Zou, D. T. Laskowitz, T.J. Huang, Acoustofluidic separation enables early diagnosis of traumatic brain injury based on circulating exosomes, Microsyst. Nanoeng. 7 (2021) 20.
[131] Z. Ma, D.J. Collins, J. Guo, Y. Ai, Mechanical properties based particle separation via traveling surface acoustic wave, Anal. Chem. 88 (2016) 11844–11851.
[132] Y. Gao, M. Wu, Y. Lin, J. Xu, Acoustic microfluidic separation techniques and bioapplications: A review, Micromach.-Basel 11 (2020).
[133] Y. Fan, X. Wang, J. Ren, F. Lin, J. Wu, Recent advances in acoustofluidic separation technology in biology, Microsyst. Nanoeng. 8 (2022) 94.
[134] Z. Ma, D.J. Collins, Y. Ai, Single-actuator bandpass microparticle filtration via traveling surface acoustic waves, colloid and interface science, Communications 16 (2017) 6–9.
[135] X. Bai, S. Bin, D. Yuguo, Z. Wei, F. Yanmin, C. Yuanyuan, Z. Deyuan, A. Fumihito, F. Lin, Parallel trapping, patterning, separating and rotating of micro-objects with various sizes and shapes using acoustic microstreaming, Sens. Actuators, A 315 (2020) e112340.
[136] X. Bai, B. Song, Z. Chen, W. Zhang, D. Chen, Y. Dai, S. Liang, D. Zhang, Z. Zhao, L. Feng, Postoperative evaluation of tumours based on label-free acoustic separation of circulating tumour cells by microstreaming, Lab Chip 21 (2021) 2721–2729.
[137] H. Qiu, H. Wang, X. Yang, F. Huo, High performance isolation of circulating tumor cells by acoustofluidic chip coupled with ultrasonic concentrated energy transducer, Colloids Surf. B Biointerfaces 222 (2023), 113138.
[138] Q.T. Xiaomin Qia, P. Liua, I.V. Mininc, O.V. Mininc, H.u. Junhui, Controlled concentration and transportation of nanoparticles at the interface between a plain substrate and droplet, Sens. Actuators B 274 (2018) 381–392.
[139] A.G. Guex, N. Di Marzio, D. Eglin, M. Alini, T. Serra, The waves that make the pattern: a review on acoustic manipulation in biomedical research, Mater Today Bio 10 (2021), 100110.
[140] L. Zwi-Dantsis, B. Wang, C. Marijon, S. Zonetti, A. Ferrini, L. Massi, D.J. Stuckey, C.M. Terracciano, M.M. Stevens, Remote magnetic nanoparticle manipulation enables the dynamic patterning of cardiac tissues, Adv. Mater. 32 (2020) e1904598.
[141] H. Tan, H. Hu, L. Huang, K. Qian, Plasmonic tweezers for optical manipulation and biomedical applications, Analyst 145 (2020) 5699–5712.
[142] A. Martinez-Rivas, G. González-Quijano, S. Proa-Coronado, C. Séverac, E. Dague, Methods of micropatterning and manipulation of cells for biomedical applications, Micromachines (Basel) 8 (12) (2017) 347.
[143] Z. Ma, A.W. Holle, K. Melde, T. Qiu, K. Poeppel, V.M. Kadiri, P. Fischer, Acoustic holographic cell patterning in a biocompatible hydrogel, Adv. Mater. 32 (2020) e1904181.
[144] S. Cohen, H. Sazan, A. Kenigsberg, H. Schori, S. Piperno, H. Shpaisman, O. Shefi, Large-scale acoustic-driven neuronal patterning and directed outgrowth, Sci. Rep. 10 (2020) 4932.
[145] D.V. Deshmukh, P. Reichert, J. Zvick, C. Labouesse, V. Künzli, O. Dudaryeva, O. Bar-Nur, M.W. Tibbitt, J. Dual, Continuous production of acoustically patterned cells within hydrogel fibers for musculoskeletal tissue engineering, Adv. Funct. Mater. 32 (30) (2022) 2113038.
[146] Y. Sriphutkiat, S. Kasetsirikul, D. Ketpun, Y. Zhou, Cell alignment and accumulation using acoustic nozzle for bioprinting, Sci. Rep. 9 (2019) 17774.
[147] P.u. Chen, S. Güven, O.B. Usta, M.L. Yarmush, U. Demirci, Biotunable acoustic node assembly of organoids, Adv. Healthc. Mater. 4 (13) (2015) 1937–1943.
[148] P.u. Chen, Z. Luo, S. Güven, S. Tasoglu, A.V. Ganesan, A. Weng, U. Demirci, Microscale assembly directed by liquid-based template, Adv. Mater. 26 (34) (2014) 5936–5941.
[149] L. Gu, S. Jiang, X. Xu, J. Wang, F. Xu, H. Fan, J. Shang, K. Liu, U. Demirci, P. u. Chen, Size- and density-dependent acoustic differential bioassembly of spatially-defined heterocellular architecture, Biofabrication 15 (1) (2023) 015019.
[150] H. Bachman, Y. Gu, J. Rufo, S. Yang, Z. Tian, P.-H. Huang, L. Yu, T.J. Huang, Low-frequency flexural wave based microparticle manipulation, Lab Chip 20 (7) (2020) 1281–1289.
[151] C. Bouyer, P. Chen, S. Guven, T.T. Demirtas, T.J. Nieland, F. Padilla, U. Demirci, A bio-acoustic levitational (BAL) assembly method for engineering of multilayered, 3D brain-like constructs, using human embryonic stem cell derived neuro-progenitors, Adv. Mater. 28 (2016) 161–167.
[152] S.-H. Hong, J.-B. Gorce, H. Punzmann, N. Francois, M. Shats, H. Xia, Surface waves control bacterial attachment and formation of biofilms in thin layers, Sci. Adv. 6 (22) (2020).
[153] A. Aghakhani, H. Cetin, P. Erkoc, G.I. Tombak, M. Sitti, Flexural wave-based soft attractor walls for trapping microparticles and cells, Lab Chip 21 (2021) 582–596.
[154] J. Zhang, S. Yang, C. Chen, J.H. Hartman, P.-H. Huang, L. Wang, Z. Tian, P. Zhang, D. Faulkenberry, J.N. Meyer, Surface acoustic waves enable rotational manipulation of Caenorhabditis elegans, Lab Chip 19 (2019) 984–992.
[155] A. Ozcelik, N. Nama, P.H. Huang, M. Kaynak, M.R. McReynolds, W. Hanna-Rose, T.J. Huang, Acoustofluidic rotational manipulation of cells and organisms using oscillating solid structures, Small 12 (2016) 5120–5125.
[156] T. Hayakawa, S. Sakuma, F. Arai, On-chip 3D rotation of oocyte based on a vibration-induced local whirling flow, Microsyst. Nanoeng. 1 (2015).
[157] Y. Zhou, J. Liu, J. Yan, S. Guo, T. Li, Soft-contact acoustic microgripper based on a controllable gas-liquid interface for biomicromanipulations, Small 17 (2021) e2104579.
[158] N.F. Laubli, J.T. Burri, J. Marquard, H. Vogler, G. Mosca, N. Vertti-Quintero, N. Shamsudhin, A. deMello, U. Grossniklaus, D. Ahmed, B.J. Nelson, 3D mechanical characterization of single cells and small organisms using acoustic manipulation and force microscopy, Nat. Commun. 12 (2021) 2583.
[159] N.F. Laubli, M.S. Gerlt, A. Wuthrich, R.T.M. Lewis, N. Shamsudhin, U. Kutay, D. Ahmed, J. Dual, B.J. Nelson, Embedded microbubbles for acoustic manipulation of single cells and microfluidic applications, Anal. Chem. 93 (2021) 9760–9770.
[160] Z. Ma, Y. Zhou, F. Cai, L. Meng, H. Zheng, Y. Ai, Ultrasonic microstreaming for complex-trajectory transport and rotation of single particles and cells, Lab Chip 20 (2020) 2947–2953.
[161] L. Feng, B. Song, Y. Chen, S. Liang, Y. Dai, Q. Zhou, D. Chen, X. Bai, Y. Feng, Y. Jiang, D. Zhang, F. Arai, On-chip rotational manipulation of microbeads and oocytes using acoustic microstreaming generated by oscillating asymmetrical microstructures, Biomicrofluidics 13 (2019), 064103.
[162] T. Hayakawa, F. Arai, On-chip micromanipulation method based on mode switching of vibration-induced asymmetric flow, in: 2017 IEEE International Conference on Robotics and Automation (ICRA), 2017, pp. 6631–6636.
[163] X. Liu, Q. Shi, Y. Lin, M. Kojima, Y. Mae, T. Fukuda, Q. Huang, T. Arai, Multifunctional noncontact micromanipulation using whirling flow generated by vibrating a single piezo actuator, Small 15 (2019) 1804421.
[164] D. Ahmed, A. Ozcelik, N. Bojanala, N. Nama, A. Upadhyay, Y. Chen, W. Hanna-Rose, T.J. Huang, Rotational manipulation of single cells and organisms using acoustic waves, Nat. Commun. 7 (2016) 11085.
[165] Y. Li, X. Liu, Q. Huang, T. Arai, Controlled rotation of micro-objects using acoustically driven microbubbles, Appl. Phys. Lett. 118 (2021), 063701.
[166] Q. Tang, F. Liang, L. Huang, P. Zhao, W. Wang, On-chip simultaneous rotation of large-scale cells by acoustically oscillating bubble array, Biomed. Microdevices 22 (2020) 13.
[167] A.J. Chung, D. Kim, D. Erickson, Electrokinetic microfluidic devices for rapid, low power drug delivery in autonomous microsystems, Lab Chip 8 (2) (2008) 330–338.
[168] S.K. Srivastava, G. Clergeaud, T.L. Andresen, A. Boisen, Micromotors for drug delivery in vivo: The road ahead, Adv. Drug Deliv. Rev. 138 (2019) 41–55.
[169] M. Kaynak, A. Ozcelik, A. Nourhani, P.E. Lammert, V.H. Crespi, T.J. Huang, Acoustic actuation of bioinspired microswimmers, Lab Chip 17 (3) (2017) 395–400.
[170] C. Dillinger, N. Nama, D. Ahmed, Ultrasound-activated ciliary bands for microrobotic systems inspired by starfish, Nat. Commun. 12 (2021) 6455.
[171] N. Bertin, T.A. Spelman, O. Stephan, L. Gredy, M. Bouriau, E. Lauga, P. Marmottant, Propulsion of bubble-based acoustic microswimmers, Phys. Rev. Appl 4 (6) (2015).
[172] T. Luo, M. Wu, Biologically inspired micro-robotic swimmers remotely controlled by ultrasound waves, Lab Chip 21 (2021) 4095–4103.
[173] A. Aghakhani, O. Yasa, P. Wrede, M. Sitti, Acoustically powered surface-slipping mobile microrobots, PNAS 117 (2020) 3469–3477.
[174] M. Arora, C.D. Ohl, K.A. Morch, Cavitation inception on microparticles: a self-propelled particle accelerator, Phys. Rev. Lett. 92 (2004), 174501.
[175] Y. Zhou, H. Wang, Z. Ma, J.K.W. Yang, Y. Ai, Acoustic vibration-induced actuation of multiple microrotors in microfluidics, Adv. Mater. Technol. (2020).
[176] M. Kaynak, P. Dirix, M.S. Sakar, Addressable acoustic actuation of 3D printed soft robotic microsystems, Adv. Sci. (Weinh) 7 (20) (2020) 2001120.
[177] X. Lu, F. Soto, J. Li, T. Li, Y. Liang, J. Wang, Topographical manipulation of microparticles and cells with acoustic microstreaming, ACS Appl. Mater. Interfaces 9 (44) (2017) 38870–38876.
[178] D. Ahmed, M. Lu, A. Nourhani, P.E. Lammert, Z. Stratton, H.S. Muddana, V. H. Crespi, T.J. Huang, Selectively manipulable acoustic-powered microswimmers, Sci. Rep. 5 (2015) 9744.
[179] D. Ahmed, T. Baasch, B. Jang, S. Pane, J. Dual, B.J. Nelson, Artificial swimmers propelled by acoustically activated flagella, Nano Lett. 16 (8) (2016) 4968–4974.
[180] X. Lu, H. Shen, Y. Wei, H. Ge, J. Wang, H. Peng, W. Liu, Ultrafast growth and locomotion of dandelion-like microswarms with tubular micromotors, Small 16 (38) (2020) 2003678.
[181] T.A. Spelman, O. Stephan, P. Marmottant, Multi-directional bubble generated streaming flows, Ultrasonics 102 (2020), 106054.
[182] T. Qiu, S. Palagi, A.G. Mark, K. Melde, F. Adams, P. Fischer, Active acoustic surfaces enable the propulsion of a wireless robot, Adv. Mater. Interfaces 4 (21) (2017) 1700933.
[183] A. Aghakhani, A. Pena-Francesch, U. Bozuyuk, H. Cetin, P. Wrede, M. Sitti, High shear rate propulsion of acoustic microrobots in complex biological fluids, Sci. Adv. 8 (10) (2022).

[184] L. Ren, N. Nama, J.M. McNeill, F. Soto, Z. Yan, W.u. Liu, W. Wang, J. Wang, T. E. Mallouk, 3D steerable, acoustically powered microswimmers for single-particle manipulation, Sci. Adv. 5 (10) (2019).
[185] X. Bai, W. Zhang, Y. Dai, Y. Wang, H. Sun, L. Feng, Acoustic and magnetic hybrid actuated immune cell robot for target and kill cancer cells, in: 2022 International Conference on Robotics and Automation (ICRA), 2022, pp. 7936–7941.
[186] Q. Gao, Z. Yang, R. Zhu, J. Wang, P. Xu, J. Liu, X. Chen, Z. Yan, Y. Peng, Y. Wang, H. Zheng, F. Cai, W. Wang, Ultrasonic steering wheels: turning micromotors by localized acoustic microstreaming, ACS Nano 17 (2023) 4729–4739.
[187] B.M. Borkent, M. Arora, C.-D. Ohl, N. De Jong, M. Versluis, D. Lohse, K.A. MØRch, E. Klaseboer, B.C. Khoo, The acceleration of solid particles subjected to cavitation nucleation, J. Fluid Mech. 610 (2008) 157–182.
[188] M. Kaynak, A. Ozcelik, N. Nama, A. Nourhani, P.E. Lammert, V.H. Crespi, T. J. Huang, Acoustofluidic actuation of in situ fabricated microrotors, Lab Chip 16 (2016) 3532–3537.
[189] D. Jang, J. Jeon, S.K. Chung, Acoustic bubble-powered miniature rotor for wireless energy harvesting in a liquid medium, Sens. Actuators, A 276 (2018) 296–303.
[190] O. Dincel, T. Ueta, J. Kameoka, Acoustic driven microbubble motor device, Sens. Actuators, A 295 (2019) 343–347.
[191] T. Qiu, F. Adams, S. Palagi, K. Melde, A. Mark, U. Wetterauer, A. Miernik, P. Fischer, Wireless Acoustic-Surface Actuators for Miniaturized Endoscopes, ACS Appl. Mater. Interfaces 9 (49) (2017) 42536–42543.
[192] X. Lu, K. Zhao, H. Peng, H. Li, W. Liu, Local Enhanced Microstreaming for Controllable High-Speed Acoustic Rotary Microsystems, Phys. Rev. Appl 11 (4) (2019).
[193] H. Shen, K. Zhao, Z. Wang, X. Xu, J. Lu, W. Liu, X. Lu, Local acoustic fields powered assembly of microparticles and applications, Micromachines (Basel) 10 (12) (2019) 882.
[194] X. Lu, K. Zhao, W. Liu, D. Yang, H. Shen, H. Peng, X. Guo, J. Li, J. Wang, A Human microrobot interface based on acoustic manipulation, ACS Nano 13 (10) (2019) 11443–11452.
[195] Y. Wei, X. Lu, H. Shen, H. Peng, Z. Yuan, X. Guo, W. Liu, An acousto-microrobotic interface with vision-feedback control, Adv. Mater. Technol. 6 (12) (2021), 2100470.
[196] D. Ahmed, T. Baasch, N. Blondel, N. Laubli, J. Dual, B.J. Nelson, Neutrophil-inspired propulsion in a combined acoustic and magnetic field, Nat. Commun. 8 (2017) 770.
[197] X. Liu, J. Li, L. Zhang, X. Huang, U. Farooq, N.a. Pang, W. Zhou, L. Qi, L. Xu, L. Niu, L. Meng, Cell Lysis Based on an Oscillating Microbubble Array, Micromachines (Basel) 11 (3) (2020) 288.
[198] A. Pourabed, T. Chakkumpulakkal Puthan Veettil, C. Devendran, P. Nair, B. R. Wood, T. Alan, A star shaped acoustofluidic mixer enhances rapid malaria diagnostics via cell lysis and whole blood homogenisation in 2 seconds, Lab Chip 22 (2022) 1829–1840.
[199] B. Song, W. Zhang, X. Bai, L. Feng, D. Zhang, F. Arai, A novel portable cell sonoporation device based on open-source acoustofluidics, in: 2020 IEEE/RSJ International Conference on Intelligent Robots and Systems (IROS), 2020, pp. 2786–2791.
[200] Y. Xie, N. Nama, P. Li, Z. Mao, P.H. Huang, C. Zhao, F. Costanzo, T.J. Huang, Probing cell deformability via acoustically actuated bubbles, Small 12 (2016) 902–910.
[201] X. Liu, W. Zhang, U. Farooq, N. Rong, J. Shi, N. Pang, L. Xu, L. Niu, L. Meng, Rapid cell pairing and fusion based on oscillating bubbles within an acoustofluidic device, Lab Chip 22 (2022) 921–927.
[202] Z. Wang, P.H. Huang, C. Chen, H. Bachman, S. Zhao, S. Yang, T.J. Huang, Cell lysis via acoustically oscillating sharp edges, Lab Chip 19 (2019) 4021–4032.
[203] M. Wang, Y. Zhang, C. Cai, J. Tu, X. Guo, D. Zhang, Sonoporation-induced cell membrane permeabilization and cytoskeleton disassembly at varied acoustic and microbubble-cell parameters, Sci. Rep. 8 (2018) 3885.
[204] X. Guo, C. Cai, G. Xu, Y. Yang, J. Tu, P. Huang, D. Zhang, Interaction between cavitation microbubble and cell: A simulation of sonoporation using boundary element method (BEM), Ultrason. Sonochem. 39 (2017) 863–871.
[205] J. Tu, A.C.H. Yu, Ultrasound-mediated drug delivery: sonoporation mechanisms, biophysics, and critical factors, BME Front. 2022 (2022).
[206] J. Rich, Z. Tian, T.J. Huang, Sonoporation: past, present, and future, Adv Mater Technol 7 (2022).
[207] C.S. Centner, E.M. Murphy, M.C. Priddy, J.T. Moore, B.R. Janis, M.A. Menze, A. P. DeFilippis, J.A. Kopechek, Ultrasound-induced molecular delivery to erythrocytes using a microfluidic system, Biomicrofluidics 14 (2020), 024114.
[208] L. Meng, F. Cai, P. Jiang, Z. Deng, F. Li, L. Niu, Y. Chen, J. Wu, H. Zheng, On-chip targeted single cell sonoporation with microbubble destruction excited by surface acoustic waves, Appl. Phys. Lett. 104 (7) (2014) 073701.
[209] L. Meng, X. Liu, Y. Wang, W. Zhang, W. Zhou, F. Cai, F. Li, J. Wu, L. Xu, L. Niu, H. Zheng, Sonoporation of cells by a parallel stable cavitation microbubble array, Adv. Sci. (Weinh) 6 (2019) 1900557.
[210] M. Eck, R. Aronovich, T. Ilovitsh, Efficacy optimization of low frequency microbubble-mediated sonoporation as a drug delivery platform to cancer cells, Int. J. Pharm. X 4 (2022), 100132.
[211] A. Salari, S. Appak-Baskoy, I.R. Coe, J. Abousawan, C.N. Antonescu, S.S.H. Tsai, M.C. Kolios, Dosage-controlled intracellular delivery mediated by acoustofluidics for lab on a chip applications, Lab Chip 21 (2021) 1788–1797.
[212] R. Song, C. Zhang, F. Teng, J. Tu, X. Guo, Z. Fan, Y. Zheng, D. Zhang, Cavitation-facilitated transmembrane permeability enhancement induced by acoustically vaporized nanodroplets, Ultrason. Sonochem. 79 (2021), 105790.
[213] Y. Yang, Q. Li, X. Guo, J. Tu, D. Zhang, Mechanisms underlying sonoporation: Interaction between microbubbles and cells, Ultrason. Sonochem. 67 (2020) 105096.
[214] Y. Gao, M. Wu, B.I. Gaynes, R.S. Dieter, J. Xu, Study of ultrasound thrombolysis using acoustic bubbles in a microfluidic device, Lab Chip 21 (2021) 3707–3714.
[215] J. Gao, C. Li, D. Xu, P. Wu, W. Lin, X. Wang, The mechanism of ultrasonic irradiation effect on viscosity variations of heavy crude oil, Ultrason. Sonochem. 81 (2021), 105842.
[216] X. Wu, G. Xu, J. Wang, Ultrasound-assisted coagulation for Microcystis aeruginosa removal using Fe3O4-loaded carbon nanotubes, RSC Adv. 10 (2020) 13525–13531.
[217] H. Kiani, Z. Zhang, D.W. Sun, Experimental analysis and modeling of ultrasound assisted freezing of potato spheres, Ultrason. Sonochem. 26 (2015) 321–331.
[218] R. Zhu, S. Jiang, D. Li, C.L. Law, Y. Han, Y. Tao, H. Kiani, D. Liu, Dehydration of apple slices by sequential drying pretreatments and airborne ultrasound-assisted air drying: Study on mass transfer, profiles of phenolics and organic acids and PPO activity, Innov. Food Sci. Emerg. Technol. 75 (2022).
[219] Y. Li, Y. Cheng, Z. Zhang, Y. Wang, B.K. Mintah, M. Dabbour, H. Jiang, R. He, H. Ma, Modification of rapeseed protein by ultrasound-assisted pH shift treatment: Ultrasonic mode and frequency screening, changes in protein solubility and structural characteristics, Ultrason. Sonochem. 69 (2020), 105240.
[220] C. Zhang, F. Teng, J. Tu, D. Zhang, L. Annunziato, Ultrasound-enhanced protective effect of tetramethylpyrazine against cerebral ischemia/reperfusion injury, PLoS One 9 (11) (2014) e113673.
[221] L. Weng, L. Li, K. Zhao, T. Xu, Y. Mao, H. Shu, X. Chen, J. Chen, J. Wu, X. Guo, J. Tu, D. Zhang, W. Sun, X. Kong, Non-invasive local acoustic therapy ameliorates diabetic heart fibrosis by suppressing ACE-mediated oxidative stress and inflammation in cardiac fibroblasts, Cardiovasc. Drugs Ther. 36 (2022) 413–424.
[222] G. Guo, L. Lu, H. Ji, Y. Ma, R. Dong, J. Tu, X. Guo, Y. Qiu, J. Wu, D. Zhang, Low intensity pulse ultrasound stimulate chondrocytes growth in a 3-D alginate scaffold through improved porosity and permeability, Ultrasonics 58 (2015) 43–52.
[223] Y. Zhou, Z. Ma, Y. Ai, Submicron Particle Concentration and Patterning with Ultralow Frequency Acoustic Vibration, Anal Chem 92 (2020) 12795–12800.